



HAL
open science

Spontaneous moisture-driven formation of $\text{Cs}_2\text{Pb}_{1-x}\text{M}_x\text{Cl}_2\text{I}_2$ single crystals with $\text{M} = \text{Bi, In, Ga}$ and Cr

Edouard Breniaux, Pascal Dufour, Jérôme Esvan, Sonia Mallet-Ladeira,
Andréa Balocchi, Christophe Tenaillau

► To cite this version:

Edouard Breniaux, Pascal Dufour, Jérôme Esvan, Sonia Mallet-Ladeira, Andréa Balocchi, et al.. Spontaneous moisture-driven formation of $\text{Cs}_2\text{Pb}_{1-x}\text{M}_x\text{Cl}_2\text{I}_2$ single crystals with $\text{M} = \text{Bi, In, Ga}$ and Cr . *Journal of Crystal Growth*, 2022, 584, pp.126584. 10.1016/j.jcrysgro.2022.126584 . hal-03599719

HAL Id: hal-03599719

<https://hal.science/hal-03599719>

Submitted on 7 Mar 2022

HAL is a multi-disciplinary open access archive for the deposit and dissemination of scientific research documents, whether they are published or not. The documents may come from teaching and research institutions in France or abroad, or from public or private research centers.

L'archive ouverte pluridisciplinaire **HAL**, est destinée au dépôt et à la diffusion de documents scientifiques de niveau recherche, publiés ou non, émanant des établissements d'enseignement et de recherche français ou étrangers, des laboratoires publics ou privés.



Open Archive Toulouse Archive Ouverte (OATAO)

OATAO is an open access repository that collects the work of Toulouse researchers and makes it freely available over the web where possible

This is an author's version published in: <http://oatao.univ-toulouse.fr/28894>

Official URL: <https://doi.org/10.1016/j.jcrysgr.2022.126584>

To cite this version:

Breniaux, Edouard^{ORCID} and Dufour, Pascal^{ORCID} and Esvan, Jérôme^{ORCID} and Mallet-Ladeira, Sonia and Balocchi, Andréa and Tenailleau, Christophe^{ORCID}
Spontaneous moisture-driven formation of Cs₂Pb_{1-x}M_xCl₂I₂ single crystals with M = Bi, In, Ga and Cr. (2022) Journal of Crystal Growth, 584. 126584.
ISSN 0022-0248

Any correspondence concerning this service should be sent to the repository administrator: tech-oatao@listes-diff.inp-toulouse.fr

Spontaneous moisture-driven formation of $\text{Cs}_2\text{Pb}_{1-x}\text{M}_x\text{Cl}_2\text{I}_2$ single crystals with $M = \text{Bi, In, Ga}$ and Cr

E. Breniaux^a, P. Dufour^a, J. Esvan^b, S. Mallet-Ladeira^c, A. Balocchi^d, C. Tenaillon^{a,*}

^a CIRIMAT, Université de Toulouse, CNRS, Université Toulouse 3 - Paul Sabatier, 118 Route de Narbonne, 31062 Toulouse cedex 9, France

^b CIRIMAT, Université de Toulouse, CNRS, INP- ENSIACET 4 allée Emile Monso - BP44362, 31030 Toulouse cedex 4, France

^c Institut de Chimie de Toulouse (UAR 2599), 118 Route de Narbonne, 31062 Toulouse Cedex 09, France

^d Université de Toulouse, INSA-CNRS-UPS, LPCNO, 135 Avenue de Rangueil, 31077 Toulouse, France

ARTICLE INFO

Communicated by Alexander Van Driessche

Keywords:

A1. Low dimensional structures
A1. X-ray diffraction
A1. Crystal structure
A2. Growth from solutions
A2. Single crystal growth
B1. Perovskites

ABSTRACT

Micrometer to millimeter platelets-like single crystals of the 2D-derived perovskite structure $\text{Cs}_2\text{PbCl}_2\text{I}_2$ were synthesized by a very simple route using the humid ambient environment surrounding a DMSO solution containing the salt precursors. $\text{Cs}_2\text{Pb}_{1-x}\text{M}_x\text{Cl}_2\text{I}_2$ formation was also evidenced by single crystal X-ray diffraction, with $M = \text{Bi, Ga, In}$ and Cr . X-ray photoelectron spectroscopy (XPS) confirmed the presence of each dopant, with an amount of $x \sim 5$ ato.% for the last three materials. For the Bi-doped sample, XPS showed a larger quantity of dopant that can be due to XPS difficulty to discriminate too close elements for a few nanometers of analysis or higher concentrations in some crystals due to the affinity of both elements to integrate this structure on the same crystallographic site. A decrease of Bi concentration was determined by ion-beam and XPS simultaneous analysis. Finally, a photoluminescence (PL) peak was observed at ~ 420 nm for all samples. Peak widening and blue-shift can be ascribed to the doping, and attributed to photon recycling and radiative self-trapped states. These results show the great versatility of ionic substitution and adaptive optoelectronic properties of the 2D phase that is stable in temperature.

1. Introduction

Since their integration in a solar cell in 2009, unusual properties of halide perovskites have interested a significant part of the scientific community [1]. This large variety of materials have tunable electronic band gaps and possess a wide absorption range especially in the UV-visible-NIR regions. Halide perovskites can be prepared as powders, layers, single crystals and quantum dots. Small thicknesses of perovskite materials allow the use of flexible substrates that can be interesting for optical and electronic applications [2,3]. Small particles can easily transport photo-generated carriers to the electrodes. Moreover, halide perovskites usually possess high carrier mobility even with high defect density [4]. Indeed, defect states are usually shallow and do not act as recombination centers, that usually reduce the collected current in solar materials such as silicon [5]. However, defect engineering and passivation strategies are often discussed in the literature in order to improve power conversion efficiencies in solar cells [6,7]. On the other side, single crystals are composed of big crystalline domain with fewer defects and have diffusion lengths up to a few micrometers [8,9]. Crystals of

halide perovskites and derivatives are usually easier to manufacture than pure silicon and can also be used as strong luminescent materials for LEDs or as photodetectors [10]. Single-crystal growth processes are already well described in the literature for hybrid and inorganic halide perovskites [11–14]. With solution-based growth, millimeters sized single-crystals can be obtained. Several techniques are presented in the literature with a slow-cooling process that uses the influence of the temperature-related solubility, slow evaporation that provokes the supersaturation of precursors, or anti-solvent vapor-assisted crystallization (AVC). The latter technique consists in slowly diffusing an anti-solvent within a perovskite solution in order to induce single-crystal growth [15,16].

Low dimension or so-called « 2D » type structures have emerged in the family of halide perovskites, aiming to further stabilize photoactive phases, for instance. Such structural modification induces optoelectronic properties changes [17–20]. 2D perovskite derivative structures are often of Ruddlesden-Popper (RP) type, but Dion-Jacobson (DJ) and Alternating Cation Interlayer (ACI) are also encountered [21]. RP structures are characterized by a separation of the octahedra in one

* Corresponding author.

E-mail address: tenailleau@chimie.ups-tlse.fr (C. Tenaillon).

direction, resulting in octahedra sheets connected in two dimensions. This separation is generally obtained by the integration of large organic cations such as alkylammoniums or phenylammoniums.

Other works have shown the synthesis of highly stable and photoactive single crystals of BDAPb₄ (BDA Butyl-diammonium) or PEA₂PbBr₄ (PEA Phenyl-ethylammonium), widening the panel of applications from solar cells, transistors, X-rays or Gamma-rays photo-detectors to new visible-light communication (VLC) systems [12,22,23]. Some revolutionary work published in 2018 has even showed the flexibility of high surface single crystals of PEAPb₄ [24].

However, fewer papers are dealing with all-inorganic 2D single crystals. Li et al. have discovered a new compound Cs₂PbCl₂I₂ of the Ruddlesden-Popper structure in 2018 with $n = 1$ based on the $A_{n+1}B_nX_{3n+1}$ general formula, where A is a wide cation, B is a smaller cation and X is a halogen [25]. This 2D structure is common with oxides but strangely very unusual for all-inorganic halide perovskites. This phase has been synthesized for the first time with flame-sealed tube heated at high temperature (>500 °C) for melting and recrystallization of crystals. Recently, an AVC method was reported for the synthesis of micro-plates by diffusion of dichloromethane into dimethylformamide [26]. An injection of oleylamine halide into oleic acid has also allowed to obtain manganese-doped Cs₂PbCl₂I₂ nanoplatelets that show an increased photoluminescence and a quantum yield of 16% [27]. The introduction of a doping agent in the structure seems to be a good strategy in order to enhance photoluminescence activity, conductivity and to modify the microstructure, as shown in our recent work performed on powder samples of the bismuth-doped Cs₂PbCl₂I₂ phase [28]. In another work, we have also showed that the addition of such 2D phase prepared in solution to a 3D all-inorganic perovskite-based halide thin layer can stabilize the black form of the perovskite which is of strong interest for photovoltaics [29].

In this work, a simple spontaneous and ambient moisture-driven single crystal growth method is developed in order to stabilize different compositions of the 2D-based Cs₂PbCl₂I₂ structure. The use of naturally hygroscopic dimethylsulfoxide (DMSO) induces crystallization upon exposure to humidity in laboratory conditions, which is inspired by the AVC method. DMSO is the most convenient solvent for poorly soluble inorganic metal halide salts (with concentrations > 1 M). However, solubility of such halide salts in DMSO drastically drops as water is added to DMSO [30,31]. The reduction in solubility induces a single crystal growth over a few days in air exposure while kept in a fume hood. The partial substitution of lead was characterized by XRD and XPS. Finally, photoluminescence properties of our new single-crystals were also analyzed.

2. Materials and methods

Lead chloride (PbCl₂ 98%), cesium iodide (CsI 99,9%), bismuth chloride (BiCl₃ 98%), indium bromide (InBr₃ 99%), gallium iodide (GaI₃ 99,99%), chromium chloride (CrCl₃ 99%) and dimethylsulfoxide solvent (DMSO 99,9%) were purchased from Sigma-Aldrich.

For the Cs₂PbCl₂I₂ single-crystal synthesis, a 2D solution was prepared by dissolving 1 mmol of PbCl₂ and 2 mmol of CsI in DMSO. Each solution was then heated at 60 °C and stirred for two hours before filtration on PTFE 0.45 μm, as a precipitate is systematically observed. Stoichiometric amounts of the different salt precursors were used in order to aim at 5 mol.% of substitution on the lead structural site. The concentration of 5 mol.% substitution was chosen in order to observe an effect on the crystal lattice by XRD analysis without generating an impurity phase and influence notably the photoluminescence properties.

The vial containing the filtered solution was then left to the air under the fume hood without stirring for one to two weeks to favour single-crystal growth.

Single-crystal X-Ray Diffraction was performed at ICT Laboratory (Toulouse, France), on a BRÜKER D8-VENTURE 4 circles apparatus equipped with a Mo-source and a Triumph monochromator at 193 K,

and on a BRUKER QUAZAR diffractometer equipped with a 30 W air-cooled Mo-microfocus source. For structure refinement parameters, crystal lattice is determined using Bruker APEX software. In addition, Miller indices and intensities are extracted from the XRD pattern (image) and implemented in SHELX software. Thus, thermal agitation, atomic positions, chemical composition and electronic density are determined. The refining parameter “R” is used in order to calculate the deviation between experimental and theoretical values (See cif files in [supplementary data](#) for more information).

A ThermoScientific Kalpha X-ray Photoelectron Spectrometer (XPS) was used with an Al-source under high vacuum (5×10^{-9} mbar). The energy was fixed at 30 eV with a step of 0.1 eV for core levels and 160 eV for surveys (step of 1 eV). The spectrometer energy calibration was done using the Au 4f_{7/2} (83.9 ± 0.1 eV) and Cu 2p_{3/2} (932.8 ± 0.1 eV) photoelectron lines. XPS spectra were recorded in direct mode N (Ec) and the background signal was removed using the Shirley method.

The flood Gun was used to neutralize charge effects on the top surface.

Photoluminescence spectroscopy analysis was made at the LPCNO laboratory (Toulouse, France), with a laser excitation source at 355 nm, 1.2 ps pulse duration at a repetition frequency of 80 MHz, 0.5 μW average power and ~1 μm excitation spot diameter at room temperature. The photoluminescence signal has been recorded using a CCD camera after being dispersed by an imaging spectrometer. A low-pass filter has been used to remove the laser scattered light from the PL signal.

3. Results and discussions

One of the great advantages provided by halide perovskites lies in their ability to be soluble in certain polar organic solvents. This property opens the way to many deposition methods such as roll-to-roll, slot-die, doctor blade, spray-, dip- or spin-coating [32–36]. The liquid process, less expensive and easier to implement industrially than the techniques used for the manufacture of silicon for photovoltaics, give rise to great hopes for the development of this technology.

3.1. Synthesis of 2D single crystals at room temperature

Lead or cesium halides are soluble in polar solvents such as dimethylformamide (DMF), DMSO, gamma-butyrolactone (GBL) or acetonitrile [37]. In their early work, Li et al. obtained single crystals of the 2D phase using melting/crystallization process in a sealed tube under nitrogen at high temperature [25]. To the best of our knowledge, there was no previous work showing the solubility of this phase in a liquid for obtaining thin films or single crystals. Solubility tests were therefore carried out in two of the solvents most commonly used in the literature: DMF and DMSO. Solutions were produced by concentrating the Cs₂PbCl₂I₂ phase to the maximum in a gradual mixture from 100% DMSO to 100% DMF. For 100% DMSO, the solution concentration in Cs₂PbCl₂I₂ is estimated to 0.6 M. For a decreasing volume percentage of DMSO, the phase solubility continuously decreases to a minimum of 0.1 M for pure DMF (see [Figure S1](#)). This demonstrates the highest solubilization potential of DMSO in comparison to DMF. According to the literature, DMSO possesses a higher dipole moment (4,0 Debye) and dielectric constant (47) in comparison to DMF (3,8 Debye and 37, respectively), that can explain the higher capability for DMSO to solubilize metal halide salts [38]. Therefore, we chose to focus our work on pure DMSO solution with the maximal concentration of 0.6 M.

As DMSO is exposed to ambient moisture, the absorption of humidity will decrease the solubility of halide salts and induce crystallization over only a few days. The hygroscopic effect of DMSO exposed to ambient humidity has already been described in a previous work [39]. The absorption of water inside the solution results in the observation of a precipitate at the bottom of the vial and a change in color solution (see [Figure S2](#)).

After a couple of weeks, the vial contains a large variety of micrometers-to-millimeters sized crystals that are imaged by a stereomicroscope on Fig. 1. Two types of crystals can easily be identified: the first one possesses a square-like shape while the other is like a needle. Both crystals were characterized by single-crystal XRD at 193 K by using APEX and SHELX software (see Fig. 2) [40–42]. Each structure was clearly identified. Square-like materials crystallize in the $I4/mmm$ space group with a b 5.6437(1) and c 18.9237(5) Å and correspond to the 2D RP structure-type of $Cs_2PbCl_2I_2$, in accordance with the cell parameters from Li et al. measured at room temperature with a 5.6385 and c 18.879(4) Å. Besides the measuring temperature difference, the small mismatch between the two sets of unit cell parameters is probably related to the synthesis methods. Li et al. used a flame-sealed tube heated until precursors melt at a temperature above 500 °C, while our method is operated at ambient temperature and in normal conditions [25].

Needle-like materials crystallize in the $Cmcm$ space group with a lamellar structure. The chemical composition is $PbI_2 \cdot DMSO$, which is a solvatomorph consisting of alternating sheets of PbI_2 and DMSO. This structure results from the high coordination between iodine and DMSO that allows to form intermediary phases during the sample preparation, as shown in previous works [43–45]. Lédée observed the formation of $MAI \cdot DMF$, $MAI \cdot DMSO$ or $MAI \cdot GBL$ solvatomorphs that can challenge the $MAPbI_3$ single crystal growth process in solution. This effect can be beneficial when intermediate compounds need to be stabilized during thin film depositions. In addition, it slows down solvent evaporation and induces a better compactness of thin layers. However, these species are very unstable once taken out of the solvent and crystals amorphization quickly occurs. On the contrary, $Cs_2PbCl_2I_2$ crystals are highly stable and can remain as such for months in ambient conditions. Millimeter size of square-shape single crystals of pure 2D phase can be obtained within a couple of weeks. This shape shows that a preferential orientation along the (a,b) planes is followed during the growing process as powder XRD analysis of the large crystals evidences for the $(00\ l)$ planes essentially (see Figure S3).

3.2. Successful attempts of lead replacement in the 2D structure

Lead substitution can provoke particular changes in optoelectronic properties. Tetragonal $Cs_2PbCl_2I_2$ exists also as a partially lead-substituted compound by using manganese or fully substituted material in $Cs_2SnCl_2I_2$ [27,46]. The former is obtained by organic route mixing oleylammonium halide salt with octadecene and oleic acid, while Li and his colleagues processed the latter in a similar manner than for the lead compound (with a flame-sealed tube under nitrogen). Pb substitution with Mn in nanoplatelets increases the crystal photoluminescence through efficient excitonic and Mn $d-d$ emission while substitution by Sn decreases the bandgap. In many studies, it appears that lead substitution does not provoke major changes in structural properties but rather enhance optical properties of the 2D phase by

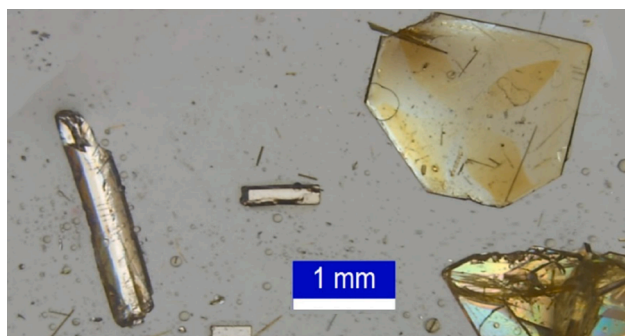


Fig. 1. Stereomicroscope image of single crystals obtained in DMSO at room temperature after a couple of weeks.

electronic band structure modification [47].

Our single crystal growth process has been used in order to prepare new 2D inorganic halide compositions while aiming at replacing lead by metals of similar size and/or oxidation states. A molar content of 5% metal was chosen to observe a significant change in the XRD pattern and avoid a compositional limitation due to steric conditions for above values. Fig. 3 shows the 2D reference and doped solutions with Bi, In, Ga and Cr, and corresponding single crystals obtained after two weeks exposure to ambient humidity. For each additive, the square-like shape of the 2D crystal is kept. Similarly to our Bi-doped 2D powders obtained earlier [28], Bi-doped 2D crystals are of reddish color, while the others are of yellowish color with Ga, In and Cr doping agents. Crystals were carefully selected from each solution and washed in oil (Fomblin YR1800) before performing further characterizations. Single-crystal XRD analysis was used in order to characterize the new crystal structures.

The unit cell and volume cell parameters of each composition are given in Fig. 4, in comparison to the undoped 2D phase. Lattice parameters and volume are always smaller in the presence of 5 ato.% of additive, strongly suggesting a substitution on the lead crystallographic site. Indeed, Pb^{2+} (ionic radius 119 pm) is the biggest cation of all elements tested (radii of Cr^{3+} 62 pm, Ga^{3+} 62 pm, In^{3+} 80 pm, Bi^{3+} 103 pm) [48]. Lead substitution by a smaller cation would then imply a unit cell volume decrease. But the unit and volume cells are almost unchanged when comparing the Cr-doped sample to the 2D reference, while Cr^{3+} radius is almost half the size of the Pb^{2+} ion. This would suggest at first that only a tiny amount of chromium ions has been integrated into the 2D phase structure or that a conjugated substitution/insertion phenomenon occurs, compensating the volume cell decrease due to substitution by intercalation of small chromium ions in interstitial sites. Similarly, a combined substitution/insertion effect could occur with Ga^{3+} due to the small size of the gallium ions, with more ions being substituted here justifying a larger volume decrease compared to the transition metal case. For In^{3+} , lead crystallographic site substitution is more effective and the volume decrease is even further evidenced for the bismuth doping, which suggests a replacement of lead on the same crystallographic site up to the full amount of bismuth introduced into the solution. Considering M^{3+} substitution for Pb^{2+} , this heterovalent-metal doping would imply an anionic excess, most probably in this case by adsorption or diffusion at the material surface rather than bulk insertion due to the large size of the anions. A second and more evident possibility is the presence of lead vacancies in the crystal structure, with the general formula expressed as $Cs_2Pb_{(1-(3/2)x)}M_x\Box_{x/2}X_4$, with $x \sim 0.05$ in our case.

X-ray photoelectron spectroscopy was used to verify each sample composition. XPS spectra are shown in Fig. 5. The peaks of Cs $3d_{5/2}$ and Cs $3d_{3/2}$ are observed at 724 and 739 eV, respectively. The $4f_{7/2}$ and $4f_{5/2}$ binding energy curves of Pb^{2+} are located at 138 and 143 eV, while small signals corresponding to similar binding energies of the Pb^0 are observed about 2 eV before each of them. These Pb metal artefacts, which can also justify the lead vacancies formed in the crystal structure, were already evidenced in halide perovskites and explained by X-ray photolysis under analytical conditions, chemical changes in air and/or the presence of PbI_2 [49]. The peaks of Cl $2p_{3/2}$ and Cl $2p_{1/2}$ are located at 198 and 200 eV while those of I $3d_{5/2}$ and I $3d_{3/2}$ are observed at 619 and 631 eV, respectively.

For each new compound, a series of specific spectral electronic orbitals characteristic of the doping agent was evidenced: Bi(4f), In(3d), Ga(3d) or Cr(2p) [50]. These orbitals, which do not interfere with any other orbitals, have thus been selected for quantification. For 5 mol. % of M doping agent, the molar ratio M/Pb should be close to 5.3%. The results are shown in Table S1. The M/Pb ratios determined after XPS analysis are comprised in between 6 and 8.6% for Ga-, In- and Cr-doped phases, slightly above the expected ratio of 5.3%. Sample cleaning and inhomogeneous distribution of the doping element throughout the whole crystal structure could explain these small discrepancies, with

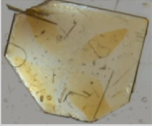
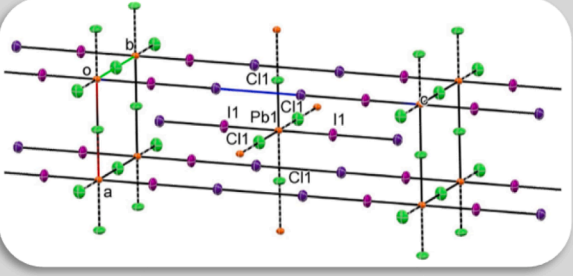

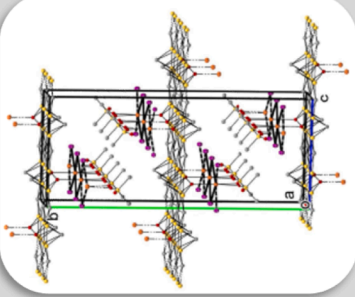
 <p>Cs₂PbCl₂I₂</p>		
<p>Structural parameters</p>	<p><i>Tetragonal - I₄/mmm</i> $a = b = 5.6437(1) \text{ \AA}$ $c = 18.9237(5) \text{ \AA}$ $\alpha = \beta = \gamma = 90^\circ$ $V = 602.75(3) \text{ \AA}^3$</p>	<p><i>Atomic positions</i> Pb (0.5 ; 0.5 ; 0.5) Cs (0 ; 0 ; 0.1306) I (0.5 ; 0.5 ; 0.3318) Cl (0.5 ; 0 ; 0.5)</p>
 <p>PbI₂.DMSO</p>		
<p>Structural parameters</p>	<p><i>Orthorhombic Cmcm</i> $a = 4.5574(4) \text{ \AA} - b = 26.552(2) \text{ \AA}$ $c = 11.1636(8) \text{ \AA}$ $\alpha = \beta = \gamma = 90^\circ$ $V = 1350.87(18) \text{ \AA}^3$</p>	

Fig. 2. Crystallographic parameters of Cs₂PbCl₂I₂ and PbI₂.DMSO single crystals obtained after X-ray diffraction analysis.

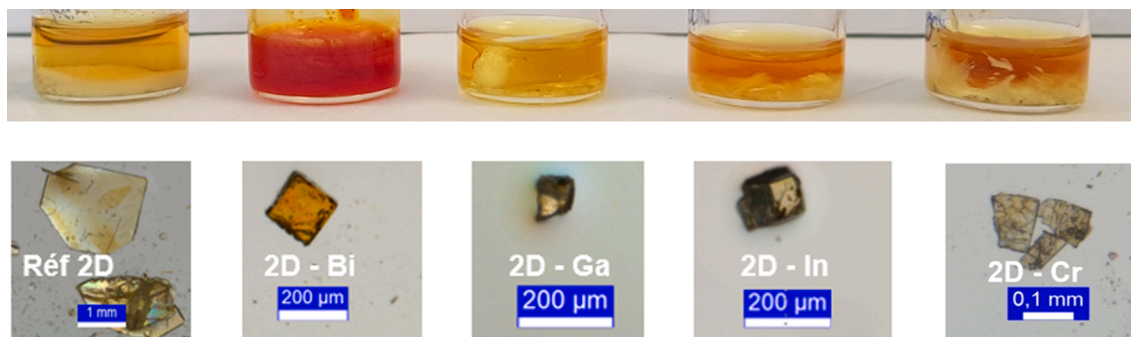


Fig. 3. Images of 2D containing solutions after a couple of weeks driving to a single-crystal growth process for (left to right) undoped (or reference material), Bi, In, Ga and Cr-doped 2D compounds and corresponding single crystals images obtained by optical microscopy.

XPS technique screening only down to a few nm from the sample surface.

For chromium doping, the peaks at binding energies of 576 and 586 eV can be assigned to the 2p_{3/2} and 2p_{1/2} of Cr in a Cr³⁺ environment. Cr⁶⁺ ions can be present in a small quantity throughout the sample as a small hump is evidenced at the base on the left hand side of each Cr³⁺ peak [51]. This phenomenon can be attributed to the ability of Cr to

form many oxidation states (+2, +3 or +6) that allows it to adapt to its chemical environment, even though the precursor introduced was CrCl₃. On the contrary, elements such as Ga, In and Bi possess a rigid +3 oxidation state that can create defects and microstrains by charge compensation effects. These effects can also explain the small lattice changes observed, in particular with Cr doping [52]. Ga 3d peaks overlap with Pb 5d and O 2s orbitals. The Ga 2p_{3/2} orbitals have two

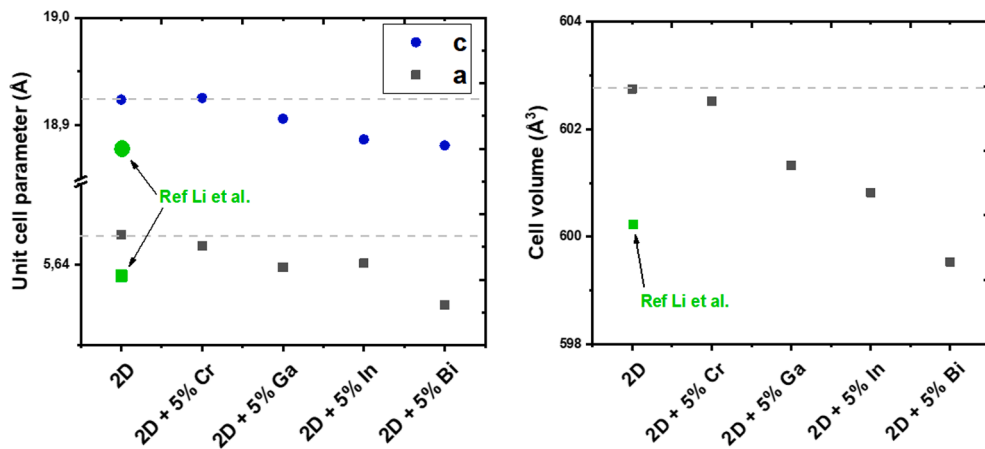


Fig. 4. Lattice parameters a and c (left) and lattice volume (right) of undoped and doped single-crystals of $\text{Cs}_2\text{Pb}_{1-x}\text{M}_x\text{Cl}_2\text{I}_2$ with $M = \text{Bi, Ga, In}$ or Cr .

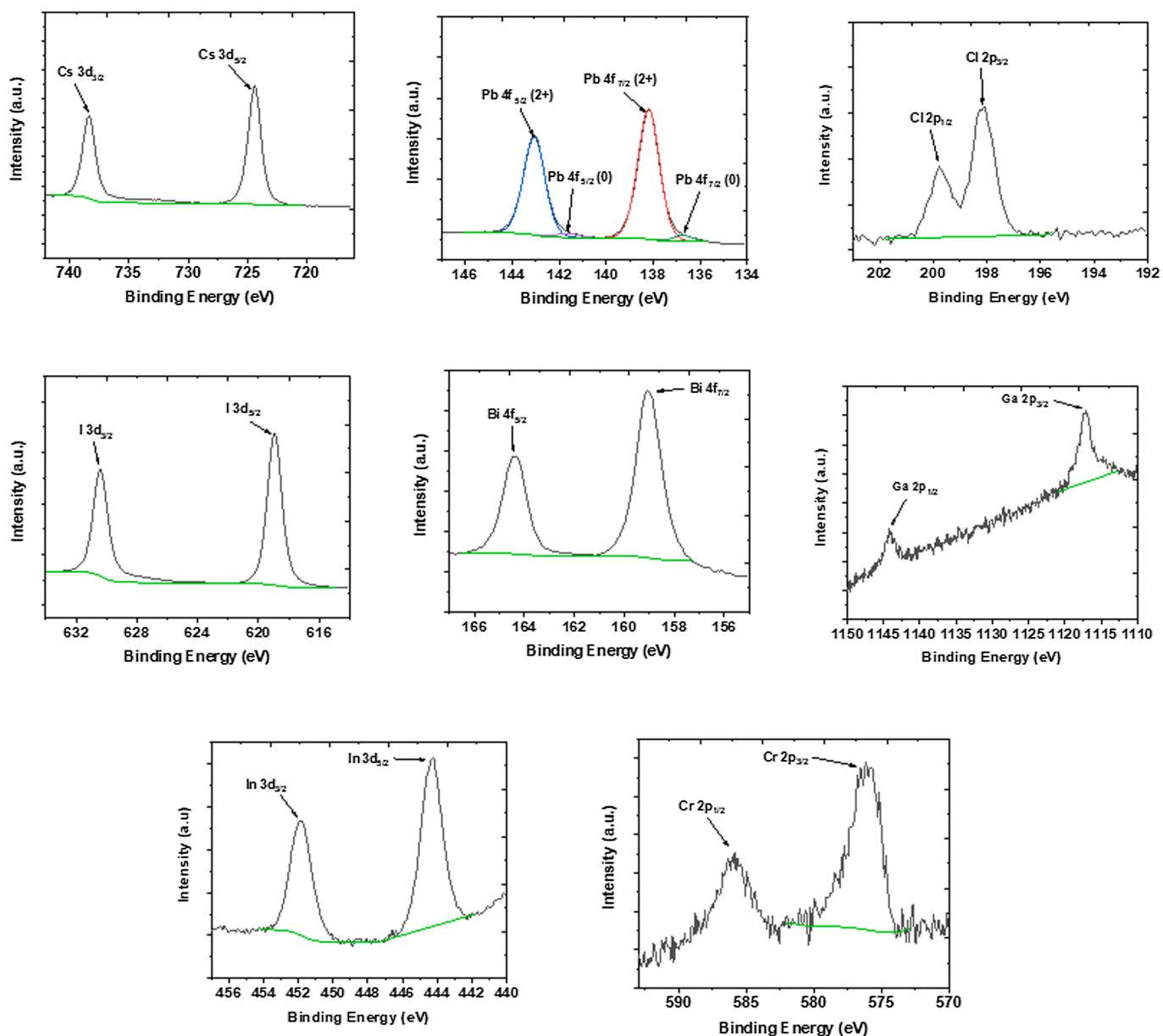


Fig. 5. Elementary orbitals obtained by XPS for the different elements in $\text{Cs}_2\text{Pb}_{1-x}\text{M}_x\text{Cl}_2\text{I}_2$ with $M = \text{Bi, Ga, In}$ or Cr .

components at 1117 and 1144 eV that might correspond to Ga metallic and +3 states, respectively [53]. For the attempt of substitution of lead by indium, we can evidence two binding energies at 445 and 452 eV in the In 3d core level XPS spectra that correspond to the spin-orbit doublets $3d_{5/2}$ and $3d_{3/2}$ of In^{3+} , respectively [54].

The largest volume contraction observed with Bi doping can be ascribed to the ability of Bi to substitute easily Pb even for larger amounts, due to steric conditions, as shown in our previous work on 2D Bi-doped powders where up to 15 at.% of bismuth could be integrated on the lead site [28]. Bismuth can thus also be present in this 2D phase prepared as a single crystal. For bismuth doping, two peaks at 159 and 164 eV can be clearly identified, which are attributed to the $4f_{7/2}$ and $4f_{5/2}$ of Bi^{3+} , respectively [55]. The quantitative analysis in this case shows a strong discrepancy between the calculated and expected values, evidencing for problems in the elemental discrimination, due to the similar electronic structures, in comparison to Pb^{2+} . Surface contaminations with salt precursors strongly bonded to the crystals even after solvent cleaning or gradient composition may as well influence the elemental quantification. In order to verify the bulk composition of the Bi-doped 2D single crystal, in-situ ionic etching has been realized with further XPS analysis (See Figure S4). This technique uses ionized argon atoms that abrade in depth the single crystal. When coupled with XPS, it allows to determine further the sample composition to at least 50 nm in depth. As etching time increases, the amounts of lead and bismuth metals increase. The increase of metallic lead content in the bulk of methylammonium lead triiodide perovskite has already been observed by Sadoughi et al. composition [56]. This effect has been correlated to the increase of the density of states in the valence band maximum, as well as an increase of defect states that reduce photoluminescence quantum efficiency of thin films. Bismuth addition is often related to reduction of crystallinity through introduction of microstrains that reduce carrier lifetime [28,57,58]. In the meantime, the total Bi/Pb ratio quickly decreases after 1 min of ion etching (from 1.1 to 0.7), which corresponds to the first 20 nm, and keeps on decreasing down to a 0.4 ratio after 6 min of etching time, corresponding to several tenth of nanometers in depth. In 2D sample powders, our previous work showed that it was possible to substitute up to about 15 mol.% of Bi in the Pb-based 2D phase, inducing large microstrains [28]. In another work performed on bismuth-doped 3D MAPbBr_3 single-crystals, compressive strains were also observed that can affect the phase compositions and transitions [59]. In our solution-based synthesis presented here, only a small amount of similar crystals was obtained and the colored crystals chosen for analysis might have contained a larger amount of bismuth than expected due a preferred selectivity of this element during the growing process.

The influence of the doping agents over the 2D single crystals optical properties was analyzed by means of photoluminescence (PL) spectroscopy operated with a 355 nm laser emission. In the UV-visible region, a maximum PL peak intensity is observed at 414 nm for the undoped $\text{Cs}_2\text{PbCl}_2\text{I}_2$ phase (Fig. 6). Similarly, a maximum peak is located at 421 nm, 416 nm and 417 nm for In-, Ga- and Cr-doped 2D phases, respectively. Full widths at half-maximum (FWHM) for each single-crystal are reported in Table S1. FWHM values systematically increase with dopant introduction. All doped samples therefore present a larger emission peak in comparison to the undoped phase, suggesting the introduction of energy levels inside the band gap of the 2D phase that increase the emission wavelengths, as described in previous works [47,60,61]. Garcia et al. calculated that new absorption peaks would be noted in Cr-doped MAPbI_3 due to in gap band (IGB) concept [47]. Our study suggests that such energy levels can also act as radiative recombination centers, as shown on the photoluminescence spectra.

Bismuth-doped 2D single-crystals exhibit two different photoluminescence peaks at 406 and 425 nm with a maximum at 406 nm. A blue shift cannot be explained by the introduction of energy levels inside the electronic gap of the 2D phase. This effect has already been observed by Wei et al. in CsPbBr_3 quantum-dots where a photoluminescence shift

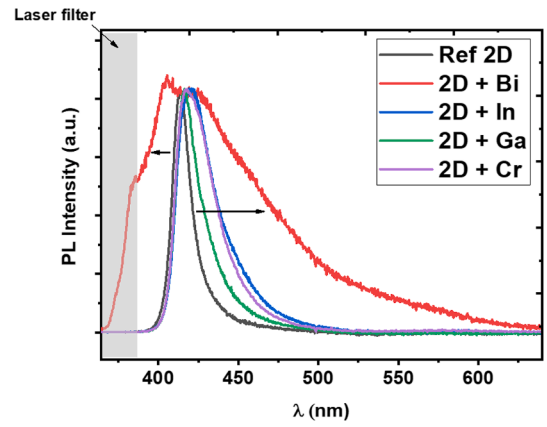


Fig. 6. UV-Visible photoluminescence spectra of $\text{Cs}_2\text{Pb}_{1-x}\text{M}_x\text{Cl}_2\text{I}_2$ single crystals with $M = \text{Bi}, \text{Ga}, \text{In}$ et Cr . Two different peaks are observed for Bi-doped single crystal, whereas only one peak is observed for all the other samples. The grey-shaded area represents the spectral range of the low-pass filter.

towards higher energies was explained by the competition between lattice expansion and exciton diffusion during the cooling stage [62]. However, PL measurements have been carried out at room temperature in our study. Yamada et al. observed a similar behavior on bismuth-doped MAPbBr_3 single crystals and explained this effect by a decrease in crystallinity that accelerates the carrier trapping rate and suppresses photon recycling [57]. This effect was also attributed to the introduction of strains and defects by bismuth ions, which we have already observed in $\text{Cs}_2\text{Pb}_{1-x}\text{Bi}_x\text{Cl}_2\text{I}_2$ powders [28]. Thus, it appears that the introduction of bismuth inside the 2D phase provokes non-trivial effects on the photoluminescence properties that are different from other additives such as In, Ga or Cr studied in this work. The introduction of such strain in the lattice is challenging for single-crystal growth but allows to enhance photoluminescence range. This particular effect can be interesting for optoelectronic applications. Since 2D phases are highly stable in normal conditions and at high temperature ($>300^\circ\text{C}$), PL measurements performed at different temperatures could also reveal more details about the structural and optical properties relationships that would enhance the importance of this 2D phase for LEDs, photovoltaics, electronic stimulators and photodetectors.

4. Conclusion

The spontaneous moisture-driven single crystal growth process has been used with an original strategy consisting in humidity absorption for preparing the all-inorganic 2D phase of $\text{Cs}_2\text{PbCl}_2\text{I}_2$ in DMSO solution. Such process is easy to operate in ambient conditions and can be performed with humidity level ranging between 30 and 60% in order to obtain up to millimeter sizes of pure crystals. Doping agents were introduced in order to prepare new 2D phases consisting of the general formula $\text{Cs}_2\text{Pb}_{0.95}\text{M}_{0.05}\text{Cl}_2\text{I}_2$ ($M = \text{Metal}$). Single crystal X-ray diffraction showed a tendency to the volume cell decrease for all-doped new 2D materials, which also exhibit a color change once doped, and X-ray photoelectron spectroscopy allowed to evidence the presence of each doping agent. The XPS semi-quantitative analysis limited to a few tenth of atomic layers revealed a doping amount close to the expected value of 5 mol%, apart from Bi-doping. In this latter case, a far higher amount was calculated, which can either be due to the complexity of elemental discrimination for Pb and Bi in this case or the selective concentration of doping agent during the single crystal growing process. Photoluminescence measurements realized at room temperature show a systematic red shift and a widening of the main emission peak under doping, probably due to the introduction of inner band gap energy levels that act as radiative energy levels. Two main intensities and a wider PL peak shifted both to lower and higher wavelengths, in the case of Bi-

doping in 2D phase can be attributed to a far more effective substitution in this case and the introduction of defects and/or strains in the crystal structure.

CRedit authorship contribution statement

E. Breniaux: Conceptualization, Project administration, Data curation, Investigation, Methodology, Writing – review & editing. **P. Dufour:** Supervision, Funding acquisition, Validation, Methodology, Writing – review & editing. **J. Esvan:** Data curation, Investigation, Methodology, Resources, Software. **S. Mallet-Ladeira:** Data curation, Investigation, Methodology, Resources, Software. **A. Balocchi:** Data curation, Investigation, Methodology, Resources, Software. **C. Tenailleau:** Conceptualization, Project administration, Data curation, Supervision, Funding acquisition, Visualization, Validation, Writing – review & editing.

Declaration of Competing Interest

The authors declare that they have no known competing financial interests or personal relationships that could have appeared to influence the work reported in this paper.

Appendix A. Supplementary data

Supplementary data to this article can be found online at <https://doi.org/10.1016/j.jcrysgro.2022.126584>.

References

- [1] A. Kojima, K. Teshima, Y. Shirai, T. Miyasaka, Organometal Halide Perovskites as Visible-Light Sensitizers for Photovoltaic Cells, *J. Am. Chem. Soc.* 131 (17) (2009) 6050–6051.
- [2] N.-G. Park, Perovskite solar cells: an emerging photovoltaic technology, *Mater. Today* 18 (2) (2015) 65–72.
- [3] W.-J. Yin, T. Shi, Y. Yan, Unique Properties of Halide Perovskites as Possible Origins of the Superior Solar Cell Performance, *Adv. Mater.* 26 (27) (2014) 4653–4658, <https://doi.org/10.1002/adma.201306281>.
- [4] S. Taheri, A. Ahmadkhan kordbacheh, M. Minbashi, A. Hajjiah, Effect of defects on high efficient perovskite solar cells, *Opt. Mater.* 111 (2021) 110601, <https://doi.org/10.1016/j.optmat.2020.110601>.
- [5] J. Kim, C.-H. Chung, K.-H. Hong, Understanding of the formation of shallow level defects from the intrinsic defects of lead tri-halide perovskites, *Phys. Chem. Chem. Phys.* 18 (39) (2016) 27143–27147.
- [6] J. Liang, X. Han, J.-H. Yang, B. Zhang, Q. Fang, J. Zhang, Q. Ai, M.M. Ogle, T. Terlier, A.A. Marti, J. Lou, Defect-Engineering-Enabled High-Efficiency All-Inorganic Perovskite Solar Cells, *Adv. Mater.* 31 (51) (2019) 1903448, <https://doi.org/10.1002/adma.v31.5110.1002/adma.201903448>.
- [7] J. Jeong, M. Kim, J. Seo, H. Lu, P. Ahlawat, A. Mishra, Y. Yang, M.A. Hope, F. T. Eickemeyer, M. Kim, Y.J. Yoon, I.W. Choi, B.P. Darwich, S.J. Choi, Y. Jo, J. H. Lee, B. Walker, S.M. Zakeeruddin, L. Emsley, U. Rothlisberger, A. Hagfeldt, D. S. Kim, M. Gratzel, J.Y. Kim, Pseudo-halide anion engineering for α -FAPbI₃ perovskite solar cells, *Nature* 592 (7854) (2021) 381–385, <https://doi.org/10.1038/s41586-021-03406-5>.
- [8] Q. Dong et al., Electron-hole diffusion lengths > 175 μ m in solution-grown CH₃NH₃PbI₃ single crystals, *Science*, 347(6225) (févr. 2015) 967–970, doi: 10.1126/science.aaa5760.
- [9] N. Giesbrecht et al., Single-crystal-like optoelectronic-properties of MAPbI₃ perovskite polycrystalline thin films, *J. Mater. Chem. A*, 6(11) (mars 2018) 4822–4828, doi: 10.1039/C7TA11190H.
- [10] S. Li, C. Zhang, J.-J. Song, X. Xie, J.-Q. Meng, S. Xu, Metal Halide Perovskite Single Crystals: From Growth Process to Application, *Crystals*, 8(5), (mai 2018) Art. no 5, doi: 10.3390/cryst8050220.
- [11] S.-S. Rong, M.B. Faheem, Y.-B. Li, Perovskite single crystals: Synthesis, properties, and applications, *J. Electron. Sci. Technol.* 19 (2) (2021) 100081, <https://doi.org/10.1016/j.jnlest.2021.100081>.
- [12] Y. Zhang, Y. Liu, Z. Xu, Z. Yang, S. (Frank) Liu, 2D Perovskite Single Crystals with Suppressed Ion Migration for High-Performance Planar-Type Photodetectors, *Small*, 16(42) (2020) 2003145, doi: <https://doi.org/10.1002/sml.202003145>.
- [13] J.-Y. Zheng, H.G. Manning, Y. Zhang, J.J. Wang, F. Purcell-Milton, A. Pokle, S.-B. Porter, C. Zhong, J. Li, R. O'Reilly Meehan, R. Enright, Y.K. Gun'ko, V. Nicolosi, J.J. Boland, S. Sanvito, J.F. Donegan, Synthesis of centimeter-size free-standing perovskite nanosheets from single-crystal lead bromide for optoelectronic devices, *Sci. Rep.* 9 (1) (2019), <https://doi.org/10.1038/s41598-019-47902-1>.
- [14] X.-D. Wang, Y.-H. Huang, J.-F. Liao, Z.-F. Wei, W.-G. Li, Y.-F. Xu, H.-Y. Chen, D.-B. Kuang, Surface passivated halide perovskite single-crystal for efficient photoelectrochemical synthesis of dimethoxydihydrofuran, *Nat. Commun.* 12 (1) (2021), <https://doi.org/10.1038/s41467-021-21487-8>.
- [15] F. Ledee, Cristallisation et fonctionnalisation de pérovskites hybrides halogénées à 2-dimensions pour le photovoltaïque et l'émission de lumière, p. 205.
- [16] Y. Dang, D. Ju, L. Wang, X. Tao, Recent progress in the synthesis of hybrid halide perovskite single crystals, *CrystEngComm* 18 (24) (2016) 4476–4484.
- [17] C.C. Stoumpos, C.M.M. Soe, H. Tsai, W. Nie, J.-C. Blancon, D.H. Cao, F. Liu, B. Traoré, C. Katan, J. Even, A.D. Mohite, M.G. Kanatzidis, High Members of the 2D Ruddlesden-Popper Halide Perovskites: Synthesis, Optical Properties, and Solar Cells of (CH₃(CH₂)₃NH₃)₂(CH₃NH₃)₄Pb₅I₁₆, *Chem* 2 (3) (2017) 427–440.
- [18] A. Shpatz Dayan, B.-E. Cohen, S. Aharon, C. Tenaillieu, M. Wierzbowska, L. Etgar, Enhancing Stability and Photostability of CsPbI₃ by Reducing Its Dimensionality, *Chem. Mater.* 30 (21) (2018) 8017–8024.
- [19] K. Wang, Z. Li, F. Zhou, H. Wang, H. Bian, H. Zhang, Q. Wang, Z. Jin, L. Ding, S. Liu, Ruddlesden-Popper 2D Component to Stabilize γ -CsPbI₃ Perovskite Phase for Stable and Efficient Photovoltaics, *Adv. Energy Mater.* 9 (42) (2019) 1902529, <https://doi.org/10.1002/aenm.v9.4210.1002/aenm.201902529>.
- [20] N. Parikh, M.M. Tavakoli, M. Pandey, M. Kumar, D. Prochowicz, R.D. Chavan, P. Yadav, Two-dimensional halide perovskite single crystals: principles and promises, *Emergent Mater.* 4 (4) (2021) 865–880, <https://doi.org/10.1007/s42247-021-00177-7>.
- [21] X. Han, Y. Zheng, S. Chai, S. Chen, et J. Xu, 2D organic-inorganic hybrid perovskite materials for nonlinear optics, *Nanophotonics*, 9(7) (juill. 2020) 1787–1810, doi: 10.1515/nanoph-2020-0038.
- [22] Y. Zhang, Y. Liu, Z. Xu, H. Ye, Q. Li, M. Hu, Z. Yang, S. (Liu), Two-dimensional (PEA)₂PbBr₄ perovskite single crystals for a high performance UV-detector, *J. Mater. Chem. C* 7 (6) (2019) 1584–1591.
- [23] J. Di, J. Chang, S. (Frank) Liu, Recent progress of two-dimensional lead halide perovskite single crystals: Crystal growth, physical properties, and device applications, *EcoMat* 2 (3) (2020) e12036, <https://doi.org/10.1002/eom2.12036>.
- [24] Y. Liu, Y. Zhang, Z. Yang, H. Ye, J. Feng, Z. Xu, X. Zhang, R. Muniir, J. Liu, P. Zuo, Q. Li, M. Hu, L. Meng, K. Wang, D.-M. Smilgies, G. Zhao, H. Xu, Z. Yang, A. Amassian, J. Li, K. Zhao, S. Liu, Multi-inch single-crystalline perovskite membrane for high-detectivity flexible photosensors, *Nat. Commun.* 9 (1) (2018), <https://doi.org/10.1038/s41467-018-07440-2>.
- [25] J. Li, Q. Yu, Y. He, C.C. Stoumpos, G. Niu, G.G. Trimarchi, H. Guo, G. Dong, D. Wang, L. Wang, M.G. Kanatzidis, Cs₂PbI₂Cl₂, All-inorganic Two-Dimensional Ruddlesden-Popper Mixed Halide Perovskite with Optoelectronic Response, *J. Am. Chem. Soc.* 140 (35) (2018) 11085–11090.
- [26] X. Li et al., Light-induced phase transition and photochromism in all-inorganic two-dimensional Cs₂PbI₂Cl₂ perovskite, *ACS Nano*, 14(8) (2020) 8.
- [27] A. Dutta, R.K. Behera, S. Deb, S. Baitalik, N. Pradhan, Doping Mn(II) in All-Inorganic Ruddlesden-Popper Phase of Tetragonal Cs₂PbCl₂ Perovskite Nanoplatelets, *J. Phys. Chem. Lett.* 10 (8) (2019) 1954–1959.
- [28] E. Breniaux, E.J. Marin-Bernardez, E. Gallet, P. Dufour, C. Tenaillieu, Synthesis and characterization of Cs₂Pb_{1-x}BixCl₂ (0 \leq x \leq 0.15) derivative perovskite, *Mater. Chem. Phys.* 247 (2020) 122870, <https://doi.org/10.1016/j.matchemphys.2020.122870>.
- [29] E. Breniaux, P. Dufour, S. Guillemet-Fritsch, C. Tenaillieu, Unraveling All-Inorganic CsPbI₃ and CsPbI₂Br Perovskite Thin Films Formation – Black Phase Stabilization by Cs₂PbI₂Cl₂ Addition and Flash-Annealing, *Eur. J. Inorg. Chem.* 2021 (30) (2021) 3059–3073, <https://doi.org/10.1002/ejic.202100304>.
- [30] Kirk-Othmer Encyclopedia of Chemical Technology, Index to Volumes 1 - 26, 5th Edition | Wiley.com. <https://www.wiley.com/en-us/Kirk+Othmer+Encyclopedia+of+Chemical+Technology%2C+Index+to+Volumes+1+26%2C+5th+Edition-p-9780471484967> (consulté le avr. 09, 2021).
- [31] B.o. Zhou, D. Ding, Y.e. Wang, S. Fang, Z. Liu, J. Tang, H. Li, H. Zhong, B. Tian, Y. Shi, A Scalable H₂O–DMF–DMSO Solvent Synthesis of Highly Luminescent Inorganic Perovskite-Related Cesium Lead Bromides, *Adv. Opt. Mater.* 9 (3) (2021) 2001435, <https://doi.org/10.1002/adom.202001435>.
- [32] Y.Y. Kim, T.-Y. Yang, R. Suhonen, A. Kemppainen, K. Hwang, N.J. Jeon, J. Seo, Roll-to-roll gravure-printed flexible perovskite solar cells using eco-friendly antisolvent bathing with wide processing window, *Nat. Commun.* 11 (1) (2020), <https://doi.org/10.1038/s41467-020-18940-5>.
- [33] Y. Zhong et al., Blade-Coated Hybrid Perovskite Solar Cells with Efficiency > 17%: An In Situ Investigation, *ACS Energy Letters*, 3(5) (mai 2018) 1078–1085, doi: 10.1021/acsenenergylett.8b00428.
- [34] M. Fievez, P.J. Singh Rana, T.M. Koh, M. Manceau, J.H. Lew, N.F. Jamaludin, B. Ghosh, A. Bruno, S. Cros, S. Berson, S.G. Mhaisalkar, W.L. Leong, Slot-die coated methylammonium-free perovskite solar cells with 18% efficiency, *Sol. Energy Mater. Sol. Cells* 230 (2021) 111189, <https://doi.org/10.1016/j.solmat.2021.111189>.
- [35] N.-G. Park, K. Zhu, Scalable fabrication and coating methods for perovskite solar cells and solar modules, *Nat. Rev. Mater.* 5 (5) (2020) 333–350.
- [36] C. Liu, Y.-B. Cheng, Z. Ge, Understanding of perovskite crystal growth and film formation in scalable deposition processes, *Chem. Soc. Rev.* 49 (6) (2020) 1653–1687, <https://doi.org/10.1039/C9CS00711C>.
- [37] E. Rezaee, W. Zhang, S.R.P. Silva, Solvent Engineering as a Vehicle for High Quality Thin Films of Perovskites and Their Device Fabrication, *Small* 17 (25) (2021) 2008145, <https://doi.org/10.1002/sml.202008145>.
- [38] W.M. Nelson, *Green Solvents for Chemistry: Perspectives and Practice*, Oxford University Press, 2003.
- [39] R. Ellison et al., In situ DMSO hydration measurements of HTS compound libraries, *Comb. Chem. High Throughput Screen.* 8(6) (sept. 2005) 489–498, doi: 10.2174/1386207054867382.
- [40] Bruker, APEX3, Bruker AXS Inc., Madison, Wisconsin, USA.

- [41] G.M. Sheldrick, SHELXT – Integrated space-group and crystal-structure determination, *Acta Crystallogr. A Found. Adv.* 71 (1) (2015) 3–8, <https://doi.org/10.1107/S2053273314026370>.
- [42] G.M. Sheldrick, Crystal structure refinement with SHELXL, *Acta Crystallogr. C Struct. Chem.* 71 (1) (2015) 3–8, <https://doi.org/10.1107/S2053229614024218>.
- [43] Y. Rong, S. Venkatesan, R. Guo, Y. Wang, J. Bao, W. Li, Z. Fan, Y. Yao, Critical kinetic control of non-stoichiometric intermediate phase transformation for efficient perovskite solar cells, *Nanoscale* 8 (26) (2016) 12892–12899.
- [44] Y. Jo, K.S. Oh, M. Kim, K.-H. Kim, H. Lee, C.-W. Lee, D.S. Kim, High Performance of Planar Perovskite Solar Cells Produced from PbI₂(DMSO) and PbI₂(NMP) Complexes by Intramolecular Exchange, *Adv. Mater. Interfaces* 3 (10) (2016) 1500768, <https://doi.org/10.1002/admi.201500768>.
- [45] Z.-W. Kwang, C.-W. Chang, T.-Y. Hsieh, T.-C. Wei, S.-Y. Lu, Solvent-modulated reaction between mesoporous PbI₂ film and CH₃NH₃I for enhancement of photovoltaic performances of perovskite solar cells, *Electrochim. Acta* 266 (2018) 118–129.
- [46] J. Li, C.C. Stoumpos, G.G. Trimarchi, I.n. Chung, L. Mao, M. Chen, M. R. Wasielewski, L. Wang, M.G. Kanatzidis, Air-Stable Direct Bandgap Perovskite Semiconductors: All-Inorganic Tin-Based Heteroleptic Halides A_xSnCl_yI_z (A Cs, Rb), *Chem. Mater.* 30 (14) (2018) 4847–4856.
- [47] G. García, P. Palacios, E. Menéndez-Proupin, A.L. Montero-Alejo, J.C. Conesa, P. Wahnón, Influence of chromium hyperdoping on the electronic structure of CH₃NH₃PbI₃ perovskite: a first-principles insight, *Sci. Rep.* 8 (1) (2018), <https://doi.org/10.1038/s41598-018-20851-x>.
- [48] R.D. Shannon, Revised effective ionic radii and systematic studies of interatomic distances in halides and chalcogenides, *Acta Crystallographica Section A* 32 (5) (1976) 751–767, <https://doi.org/10.1107/S0567739476001551>.
- [49] J.D. McGettrick, K. Hooper, A. Pockett, J. Baker, J. Troughton, M. Carnie, T. Watson, Sources of Pb(0) artefacts during XPS analysis of lead halide perovskites, *Mater. Lett.* 251 (2019) 98–101.
- [50] NIST XPS Database, <https://srdata.nist.gov/xps/ElmSpectralSrch.aspx?selEnergy PE> (consulté le oct. 21, 2021).
- [51] Y. Chen, D. An, S. Sun, J. Gao, L. Qian, Reduction and Removal of Chromium VI in Water by Powdered Activated Carbon, *Materials* 11 (2) (2018), <https://doi.org/10.3390/ma11020269>. Art. No 2.
- [52] S.I. Shupack, The chemistry of chromium and some resulting analytical problems. *Environ. Health Perspect.* 92 (1991) 7–11.
- [53] C.I.M. Rodríguez, M.Á.L. Álvarez, J.d.J.F. Rivera, G.G.C. Arizaga, C.R. Michel, α-Ga₂O₃ as a Photocatalyst in the Degradation of Malachite Green, *ECS J. Solid State Sci. Technol.* 8 (7) (2019) Q3180–Q3186.
- [54] D.V. Shinde, D.Y. Ahn, V.V. Jadhav, D.Y. Lee, N.K. Shrestha, J.K. Lee, H.Y. Lee, R. S. Mane, S.-H. Han, A coordination chemistry approach for shape controlled synthesis of indium oxide nanostructures and their photoelectrochemical properties, *J. Mater. Chem. A* 2 (15) (2014) 5490–5498.
- [55] B.o. Weng, X. Zhang, N. Zhang, Z.-R. Tang, Y.-J. Xu, Two-Dimensional MoS₂ Nanosheet-Coated Bi₂S₃ Discoids: Synthesis, Formation Mechanism, and Photocatalytic Application, *Langmuir* 31 (14) (2015) 4314–4322.
- [56] G. Sadoughi, D.E. Starr, E. Handick, S.D. Stranks, M. Gorgoi, R.G. Wilks, M. Bar, H. J. Snaith, Observation and Mediation of the Presence of Metallic Lead in Organic–Inorganic Perovskite Films, *ACS Appl. Mater. Interfaces* 7 (24) (2015) 13440–13444.
- [57] Y. Yamada, M. Hoyano, R. Akashi, K. Oto, Y. Kanemitsu, Impact of Chemical Doping on Optical Responses in Bismuth-Doped CH₃NH₃PbBr₃ Single Crystals: Carrier Lifetime and Photon Recycling, *J. Phys. Chem. Lett.* 8 (23) (2017) 5798–5803.
- [58] S. Karthick, H. Hawashin, N. Parou, S. Vedraïne, S. Velumani, J. Bouclé, Copper and Bismuth incorporated mixed cation perovskite solar cells by one-step solution process, *Sol. Energy* 218 (2021) 226–236.
- [59] E. Jedlicka, J. Wang, J. Mutch, Y.-K. Jung, P. Went, J. Mohammed, M. Ziffer, R. Giridharagopal, A. Walsh, J.-H. Chu, D.S. Ginger, Bismuth Doping Alters Structural Phase Transitions in Methylammonium Lead Tribromide Single Crystals, *J. Phys. Chem. Lett.* 12 (11) (2021) 2749–2755.
- [60] K. Kobayashi, H. Hasegawa, Y. Takahashi, J. Harada, T. Inabe, Electronic properties of tin iodide hybrid perovskites: effect of indium doping, *Mater. Chem. Front.* 2 (7) (2018) 1291–1295.
- [61] L. Presmanes et al., Ga doped ZnO thin films deposited by RF sputtering for NO₂ sensing, in: 2019 5th Experiment International Conference (exp.at'19), juin 2019, p. 454-457. doi: 10.1109/EXPAT.2019.8876525.
- [62] K. Wei, Z. Xu, R. Chen, X. Zheng, X. Cheng, T. Jiang, Temperature-dependent excitonic photoluminescence excited by two-photon absorption in perovskite CsPbBr₃ quantum dots, *Opt. Lett., OL*, 41(16) (août 2016) 3821–3824, doi: 10.1364/OL.41.003821.

Supporting Information

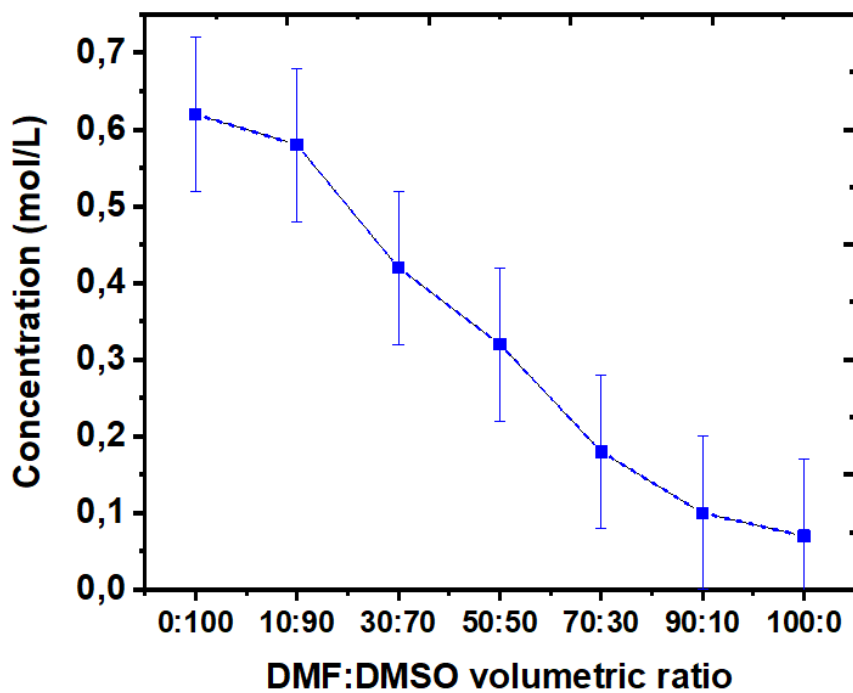


Figure S1 $\text{Cs}_2\text{PbCl}_2\text{I}_2$ solubility variation as a function of DMF/DMSO volume ratio



Figure S2 Photography of the solutions before (left) and after (right) 14 days driving to the single-crystal growth of $\text{Cs}_2\text{PbCl}_2\text{I}_2$ -type materials.

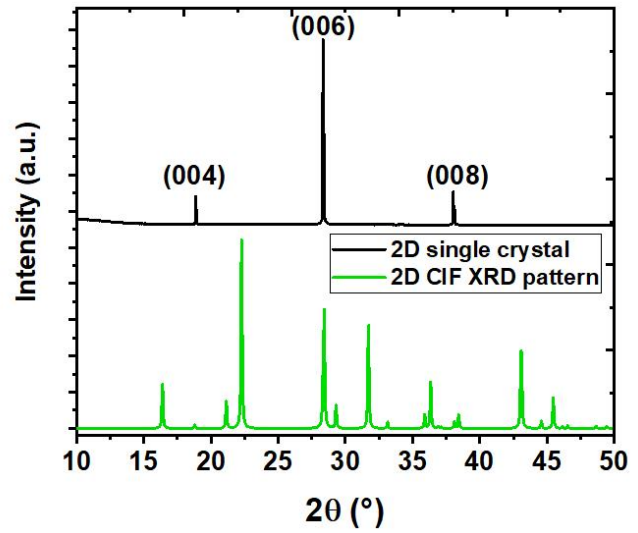
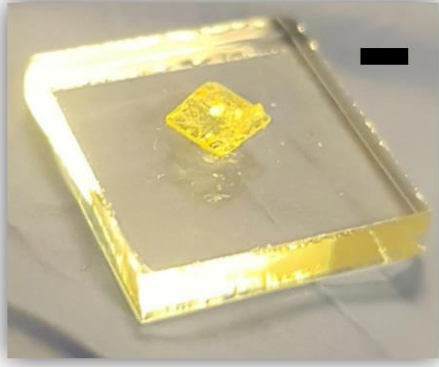


Figure S3 (Left) Photography of a 2D single-crystal (bar length = 2 mm) on a glass substrate and (right) corresponding X-ray diffraction pattern compared to the simulated theoretical CIF pattern.

Table S1 Elementary quantification of lead and M doping agent in single-crystals as determined by XPS and full width at half-maximum of the photoluminescence peak (uncertainties are $\pm 5\%$).

Sample	Pb (%)	Dopant (%)	Ratio M/Pb (%)	PL Peak FWHM (nm)
Undoped 2D ($\text{Cs}_2\text{PbCl}_2\text{I}_2$)	17.1			13
Bi-doped 2D	12.7	12.3	97	91
Ga-doped 2D	40.2	1.2	7	28
In-doped 2D	57.9	3.5	6	19
Cr-doped 2D	36.1	3.1	9	27

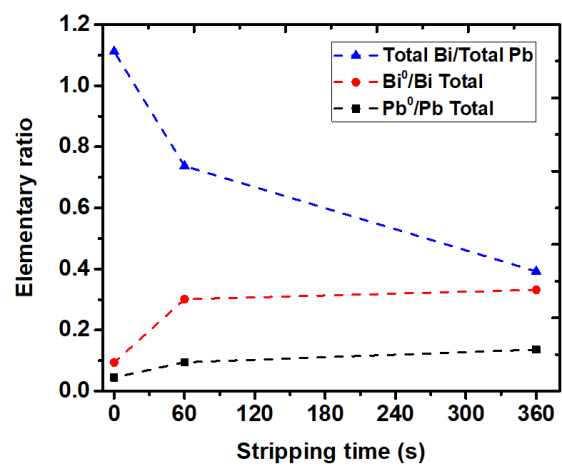


Figure S₄ Elemental proportion variation as a function of ionic etching time for a Bi-doped 2D single crystal.

The following ALERTS were generated. Each ALERT has the format

test-name_ALERT_alert-type_alert-level.

Click on the hyperlinks for more details of the test.

 **Alert level C**

PLAT242_ALERT_2_C	Low	'MainMol' Ueq as Compared to Neighbors of	Pb1	Check
PLAT911_ALERT_3_C	Missing	FCF Refl Between Thmin & STh/L= 0.600	4	Report
PLAT913_ALERT_3_C	Missing	# of Very Strong Reflections in FCF	4	Note
PLAT971_ALERT_2_C	Check	Calcd Resid. Dens. 0.89A From Pb1	1.70	eA-3
PLAT974_ALERT_2_C	Check	Calcd Negative Resid. Density on Cs1	-1.16	eA-3
PLAT974_ALERT_2_C	Check	Calcd Negative Resid. Density on Pb1	-1.03	eA-3

 **Alert level G**

PLAT004_ALERT_5_G	Polymeric	Structure Found with Maximum Dimension	2	Info
PLAT042_ALERT_1_G	Calc. and Reported	Moiety Formula Strings Differ	Please	Check
PLAT910_ALERT_3_G	Missing	# of FCF Reflection(s) Below Theta(Min).	1	Note

- 0 **ALERT level A** = Most likely a serious problem - resolve or explain
- 0 **ALERT level B** = A potentially serious problem, consider carefully
- 6 **ALERT level C** = Check. Ensure it is not caused by an omission or oversight
- 3 **ALERT level G** = General information/check it is not something unexpected

- 1 ALERT type 1 CIF construction/syntax error, inconsistent or missing data
 - 4 ALERT type 2 Indicator that the structure model may be wrong or deficient
 - 3 ALERT type 3 Indicator that the structure quality may be low
 - 0 ALERT type 4 Improvement, methodology, query or suggestion
 - 1 ALERT type 5 Informative message, check
-

checkCIF publication errors

 **Alert level A**

PUBL004_ALERT_1_A The contact author's name and address are missing, _publ_contact_author_name and _publ_contact_author_address.

PUBL005_ALERT_1_A _publ_contact_author_email, _publ_contact_author_fax and _publ_contact_author_phone are all missing.
At least one of these should be present.

PUBL006_ALERT_1_A _publ_requested_journal is missing
e.g. 'Acta Crystallographica Section C'

PUBL008_ALERT_1_A _publ_section_title is missing. Title of paper.

PUBL009_ALERT_1_A _publ_author_name is missing. List of author(s) name(s).

PUBL010_ALERT_1_A _publ_author_address is missing. Author(s) address(es).

PUBL012_ALERT_1_A _publ_section_abstract is missing.
Abstract of paper in English.

 **Alert level G**

PUBL017_ALERT_1_G The _publ_section_references section is missing or empty.

7 **ALERT level A** = Data missing that is essential or data in wrong format

1 **ALERT level G** = General alerts. Data that may be required is missing

Publication of your CIF

You should attempt to resolve as many as possible of the alerts in all categories. Often the minor alerts point to easily fixed oversights, errors and omissions in your CIF or refinement strategy, so attention to these fine details can be worthwhile. In order to resolve some of the more serious problems it may be necessary to carry out additional measurements or structure refinements. However, the nature of your study may justify the reported deviations from journal submission requirements and the more serious of these should be commented upon in the discussion or experimental section of a paper or in the "special_details" fields of the CIF. *checkCIF* was carefully designed to identify outliers and unusual parameters, but every test has its limitations and alerts that are not important in a particular case may appear. Conversely, the absence of alerts does not guarantee there are no aspects of the results needing attention. It is up to the individual to critically assess their own results and, if necessary, seek expert advice.

If level A alerts remain, which you believe to be justified deviations, and you intend to submit this CIF for publication in a journal, you should additionally insert an explanation in your CIF using the Validation Reply Form (VRF) below. This will allow your explanation to be considered as part of the review process.

Validation response form

Please find below a validation response form (VRF) that can be filled in and pasted into your CIF.

```
# start Validation Reply Form
_vrf_PUBL004_GLOBAL
;
PROBLEM: The contact author's name and address are missing,
RESPONSE: ...
;
_vrf_PUBL005_GLOBAL
;
PROBLEM: _publ_contact_author_email, _publ_contact_author_fax and
RESPONSE: ...
;
_vrf_PUBL006_GLOBAL
;
PROBLEM: _publ_requested_journal is missing
RESPONSE: ...
;
_vrf_PUBL008_GLOBAL
;
PROBLEM: _publ_section_title is missing. Title of paper.
RESPONSE: ...
;
```

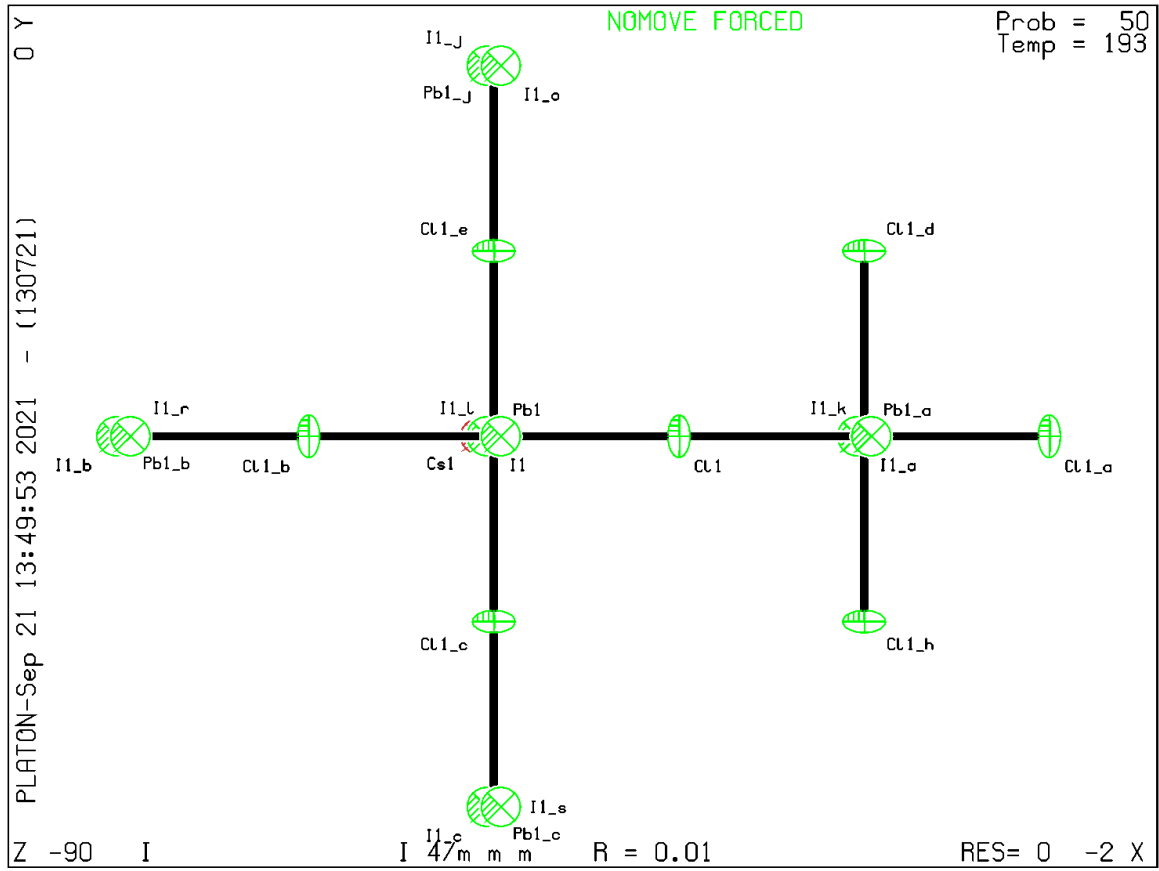


```
_vrf_PUBL009_GLOBAL
;
PROBLEM: _publ_author_name is missing. List of author(s) name(s).
RESPONSE: ...
;
_vrf_PUBL010_GLOBAL
;
PROBLEM: _publ_author_address is missing. Author(s) address(es).
RESPONSE: ...
;
_vrf_PUBL012_GLOBAL
;
PROBLEM: _publ_section_abstract is missing.
RESPONSE: ...
;
# end Validation Reply Form
```

If you wish to submit your CIF for publication in Acta Crystallographica Section C or E, you should upload your CIF via [the web](#). If you wish to submit your CIF for publication in IUCrData you should upload your CIF via [the web](#). If your CIF is to form part of a submission to another IUCr journal, you will be asked, either during electronic [submission](#) or by the Co-editor handling your paper, to upload your CIF via our web site.

PLATON version of 13/07/2021; check.def file version of 13/07/2021

Datablock I - ellipsoid plot



checkCIF/PLATON report

Structure factors have been supplied for datablock(s) I

THIS REPORT IS FOR GUIDANCE ONLY. IF USED AS PART OF A REVIEW PROCEDURE FOR PUBLICATION, IT SHOULD NOT REPLACE THE EXPERTISE OF AN EXPERIENCED CRYSTALLOGRAPHIC REFEREE.

No syntax errors found. CIF dictionary Interpreting this report

Datablock: I

Bond precision: = 0.0000 A Wavelength=0.71073

Cell: a=5.6424(1) b=5.6424(1) c=18.9253(6)
 alpha=90 beta=90 gamma=90

Temperature: 193 K

	Calculated	Reported
Volume	602.52(3)	602.52(3)
Space group	I 4/m m m	I 4/m m m
Hall group	-I 4 2	-I 4 2
Moiety formula	C14 I4 Pb1.90, 4(Cs), 0.1(Cr)	C12 Cr0.05 Cs2 I2 Pb0.95
Sum formula	C14 Cr0.10 Cs4 I4 Pb1.90	C12 Cr0.05 Cs2 I2 Pb0.95
Mr	1579.89	789.95
Dx, g cm ⁻³	4.354	4.354
Z	1	2
Mu (mm ⁻¹)	24.798	24.799
F000	658.2	658.2
F000'	649.83	
h, k, lmax	8, 8, 28	8, 8, 28
Nref	385	384
Tmin, Tmax	0.016, 0.609	0.520, 0.748
Tmin'	0.008	

Correction method= # Reported T Limits: Tmin=0.520 Tmax=0.748
AbsCorr = MULTI-SCAN

Data completeness= 0.997 Theta(max)= 33.109

R(reflections)= 0.0170(384)

wR2(reflections)=
0.0493(384)

S = 1.266

Npar= 15

The following ALERTS were generated. Each ALERT has the format
test-name_ALERT_alert-type_alert-level.

Click on the hyperlinks for more details of the test.

 **Alert level C**

PLAT077_ALERT_4_C	Unitcell Contains Non-integer Number of Atoms ..	Please Check
PLAT934_ALERT_3_C	Number of (Iobs-Icalc)/Sigma(W) > 10 Outliers ..	1 Check
PLAT972_ALERT_2_C	Check Calcd Resid. Dens. 0.37A From I1	-2.20 eA-3
PLAT974_ALERT_2_C	Check Calcd Negative Resid. Density on Cs2	-1.14 eA-3

 **Alert level G**

PLAT003_ALERT_2_G	Number of Uiso or Uij Restrained non-H Atoms ...	2 Report
PLAT004_ALERT_5_G	Polymeric Structure Found with Maximum Dimension	2 Info
PLAT042_ALERT_1_G	Calc. and Reported Moiety Formula Strings Differ	Please Check
PLAT045_ALERT_1_G	Calculated and Reported Z Differ by a Factor ...	0.50 Check
PLAT177_ALERT_4_G	The CIF-Embedded .res File Contains DELU Records	1 Report
PLAT178_ALERT_4_G	The CIF-Embedded .res File Contains SIMU Records	1 Report
PLAT300_ALERT_4_G	Atom Site Occupancy of Pb1 Constrained at	0.9499 Check
PLAT300_ALERT_4_G	Atom Site Occupancy of Cr1 Constrained at	0.0501 Check
PLAT301_ALERT_3_G	Main Residue Disorder(Resd 1)	71% Note
PLAT302_ALERT_4_G	Anion/Solvent/Minor-Residue Disorder (Resd 3)	100% Note
PLAT860_ALERT_3_G	Number of Least-Squares Restraints	6 Note
PLAT910_ALERT_3_G	Missing # of FCF Reflection(s) Below Theta(Min).	1 Note
PLAT933_ALERT_2_G	Number of OMIT Records in Embedded .res File ...	1 Note
PLAT961_ALERT_5_G	Dataset Contains no Negative Intensities	Please Check

0 **ALERT level A** = Most likely a serious problem - resolve or explain
0 **ALERT level B** = A potentially serious problem, consider carefully
4 **ALERT level C** = Check. Ensure it is not caused by an omission or oversight
14 **ALERT level G** = General information/check it is not something unexpected

2 ALERT type 1 CIF construction/syntax error, inconsistent or missing data
4 ALERT type 2 Indicator that the structure model may be wrong or deficient
4 ALERT type 3 Indicator that the structure quality may be low
6 ALERT type 4 Improvement, methodology, query or suggestion
2 ALERT type 5 Informative message, check

checkCIF publication errors

 **Alert level A**

PUBL004_ALERT_1_A The contact author's name and address are missing,
_publ_contact_author_name and _publ_contact_author_address.
PUBL005_ALERT_1_A _publ_contact_author_email, _publ_contact_author_fax and
_publ_contact_author_phone are all missing.
At least one of these should be present.
PUBL006_ALERT_1_A _publ_requested_journal is missing
e.g. 'Acta Crystallographica Section C'
PUBL008_ALERT_1_A _publ_section_title is missing. Title of paper.
PUBL009_ALERT_1_A _publ_author_name is missing. List of author(s) name(s).

PUBL010_ALERT_1_A _publ_author_address is missing. Author(s) address(es).
PUBL012_ALERT_1_A _publ_section_abstract is missing.
Abstract of paper in English.

Alert level G

PUBL017_ALERT_1_G The _publ_section_references section is missing or empty.

- 7 **ALERT level A** = Data missing that is essential or data in wrong format
 - 1 **ALERT level G** = General alerts. Data that may be required is missing
-

Publication of your CIF

You should attempt to resolve as many as possible of the alerts in all categories. Often the minor alerts point to easily fixed oversights, errors and omissions in your CIF or refinement strategy, so attention to these fine details can be worthwhile. In order to resolve some of the more serious problems it may be necessary to carry out additional measurements or structure refinements. However, the nature of your study may justify the reported deviations from journal submission requirements and the more serious of these should be commented upon in the discussion or experimental section of a paper or in the "special_details" fields of the CIF. *checkCIF* was carefully designed to identify outliers and unusual parameters, but every test has its limitations and alerts that are not important in a particular case may appear. Conversely, the absence of alerts does not guarantee there are no aspects of the results needing attention. It is up to the individual to critically assess their own results and, if necessary, seek expert advice.

If level A alerts remain, which you believe to be justified deviations, and you intend to submit this CIF for publication in a journal, you should additionally insert an explanation in your CIF using the Validation Reply Form (VRF) below. This will allow your explanation to be considered as part of the review process.

Validation response form

Please find below a validation response form (VRF) that can be filled in and pasted into your CIF.

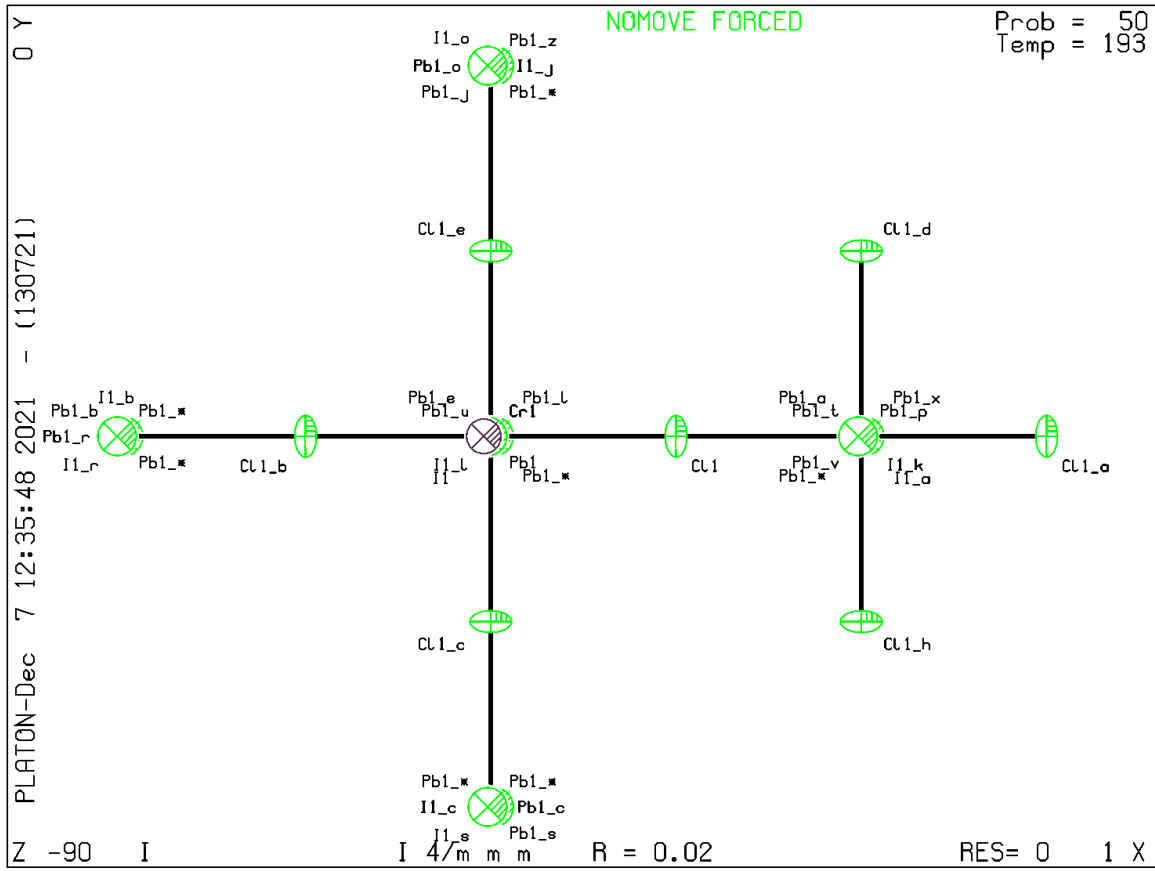
```
# start Validation Reply Form
_vrf_PUBL004_GLOBAL
;
PROBLEM: The contact author's name and address are missing,
RESPONSE: ...
;
_vrf_PUBL005_GLOBAL
;
PROBLEM: _publ_contact_author_email, _publ_contact_author_fax and
RESPONSE: ...
;
_vrf_PUBL006_GLOBAL
;
PROBLEM: _publ_requested_journal is missing
RESPONSE: ...
```

```
;
_vrf_PUBL008_GLOBAL
;
PROBLEM: _publ_section_title is missing. Title of paper.
RESPONSE: ...
;
_vrf_PUBL009_GLOBAL
;
PROBLEM: _publ_author_name is missing. List of author(s) name(s).
RESPONSE: ...
;
_vrf_PUBL010_GLOBAL
;
PROBLEM: _publ_author_address is missing. Author(s) address(es).
RESPONSE: ...
;
_vrf_PUBL012_GLOBAL
;
PROBLEM: _publ_section_abstract is missing.
RESPONSE: ...
;
# end Validation Reply Form
```

If you wish to submit your CIF for publication in Acta Crystallographica Section C or E, you should upload your CIF via [the web](#). If you wish to submit your CIF for publication in IUCrData you should upload your CIF via [the web](#). If your CIF is to form part of a submission to another IUCr journal, you will be asked, either during electronic [submission](#) or by the Co-editor handling your paper, to upload your CIF via our web site.

PLATON version of 13/07/2021; check.def file version of 13/07/2021

Datablock I - ellipsoid plot



The following ALERTS were generated. Each ALERT has the format
test-name_ALERT_alert-type_alert-level.

Click on the hyperlinks for more details of the test.

 **Alert level A**

PLAT973_ALERT_2_A	Check Calcd Positive Resid. Density on	Pb1	3.09 eA-3
PLAT973_ALERT_2_A	Check Calcd Positive Resid. Density on	Gal	3.09 eA-3

 **Alert level B**

PLAT972_ALERT_2_B	Check Calcd Resid. Dens. 0.89A	From Pb1	-2.51 eA-3
-------------------	--------------------------------	----------	------------

 **Alert level C**

PLAT077_ALERT_4_C	Unitcell Contains Non-integer Number of Atoms ..	Please Check
PLAT911_ALERT_3_C	Missing FCF Refl Between Thmin & STh/L= 0.600	26 Report
PLAT913_ALERT_3_C	Missing # of Very Strong Reflections in FCF	14 Note
PLAT972_ALERT_2_C	Check Calcd Resid. Dens. 0.99A	From Cs1 -2.40 eA-3

 **Alert level G**

PLAT003_ALERT_2_G	Number of Uiso or Uij Restrained non-H Atoms ...	2 Report
PLAT004_ALERT_5_G	Polymeric Structure Found with Maximum Dimension	2 Info
PLAT019_ALERT_1_G	_diffrn_measured_fraction_theta_full/*_max < 1.0	0.914 Report
PLAT042_ALERT_1_G	Calc. and Reported Moiety Formula Strings Differ	Please Check
PLAT045_ALERT_1_G	Calculated and Reported Z Differ by a Factor ...	0.50 Check
PLAT068_ALERT_1_G	Reported F000 Differs from Calcd (or Missing)...	Please Check
PLAT177_ALERT_4_G	The CIF-Embedded .res File Contains DELU Records	1 Report
PLAT178_ALERT_4_G	The CIF-Embedded .res File Contains SIMU Records	1 Report
PLAT300_ALERT_4_G	Atom Site Occupancy of Pb1 Constrained at	0.9499 Check
PLAT300_ALERT_4_G	Atom Site Occupancy of Gal Constrained at	0.0501 Check
PLAT301_ALERT_3_G	Main Residue Disorder(Resd 1)	71% Note
PLAT302_ALERT_4_G	Anion/Solvent/Minor-Residue Disorder (Resd 3)	100% Note
PLAT802_ALERT_4_G	CIF Input Record(s) with more than 80 Characters	2 Info
PLAT860_ALERT_3_G	Number of Least-Squares Restraints	6 Note
PLAT910_ALERT_3_G	Missing # of FCF Reflection(s) Below Theta(Min).	2 Note
PLAT961_ALERT_5_G	Dataset Contains no Negative Intensities	Please Check

2 **ALERT level A** = Most likely a serious problem - resolve or explain
1 **ALERT level B** = A potentially serious problem, consider carefully
4 **ALERT level C** = Check. Ensure it is not caused by an omission or oversight
16 **ALERT level G** = General information/check it is not something unexpected

4 ALERT type 1 CIF construction/syntax error, inconsistent or missing data
5 ALERT type 2 Indicator that the structure model may be wrong or deficient
5 ALERT type 3 Indicator that the structure quality may be low
7 ALERT type 4 Improvement, methodology, query or suggestion
2 ALERT type 5 Informative message, check

checkCIF publication errors

Alert level A

PUBL004_ALERT_1_A The contact author's name and address are missing, `_publ_contact_author_name` and `_publ_contact_author_address`.
PUBL005_ALERT_1_A `_publ_contact_author_email`, `_publ_contact_author_fax` and `_publ_contact_author_phone` are all missing.
At least one of these should be present.
PUBL006_ALERT_1_A `_publ_requested_journal` is missing
e.g. 'Acta Crystallographica Section C'
PUBL008_ALERT_1_A `_publ_section_title` is missing. Title of paper.
PUBL009_ALERT_1_A `_publ_author_name` is missing. List of author(s) name(s).
PUBL010_ALERT_1_A `_publ_author_address` is missing. Author(s) address(es).
PUBL012_ALERT_1_A `_publ_section_abstract` is missing.
Abstract of paper in English.

Alert level G

PUBL017_ALERT_1_G The `_publ_section_references` section is missing or empty.

7 **ALERT level A** = Data missing that is essential or data in wrong format
1 **ALERT level G** = General alerts. Data that may be required is missing

Publication of your CIF

You should attempt to resolve as many as possible of the alerts in all categories. Often the minor alerts point to easily fixed oversights, errors and omissions in your CIF or refinement strategy, so attention to these fine details can be worthwhile. In order to resolve some of the more serious problems it may be necessary to carry out additional measurements or structure refinements. However, the nature of your study may justify the reported deviations from journal submission requirements and the more serious of these should be commented upon in the discussion or experimental section of a paper or in the "special_details" fields of the CIF. *checkCIF* was carefully designed to identify outliers and unusual parameters, but every test has its limitations and alerts that are not important in a particular case may appear. Conversely, the absence of alerts does not guarantee there are no aspects of the results needing attention. It is up to the individual to critically assess their own results and, if necessary, seek expert advice.

If level A alerts remain, which you believe to be justified deviations, and you intend to submit this CIF for publication in a journal, you should additionally insert an explanation in your CIF using the Validation Reply Form (VRF) below. This will allow your explanation to be considered as part of the review process.

Validation response form

Please find below a validation response form (VRF) that can be filled in and pasted into your CIF.

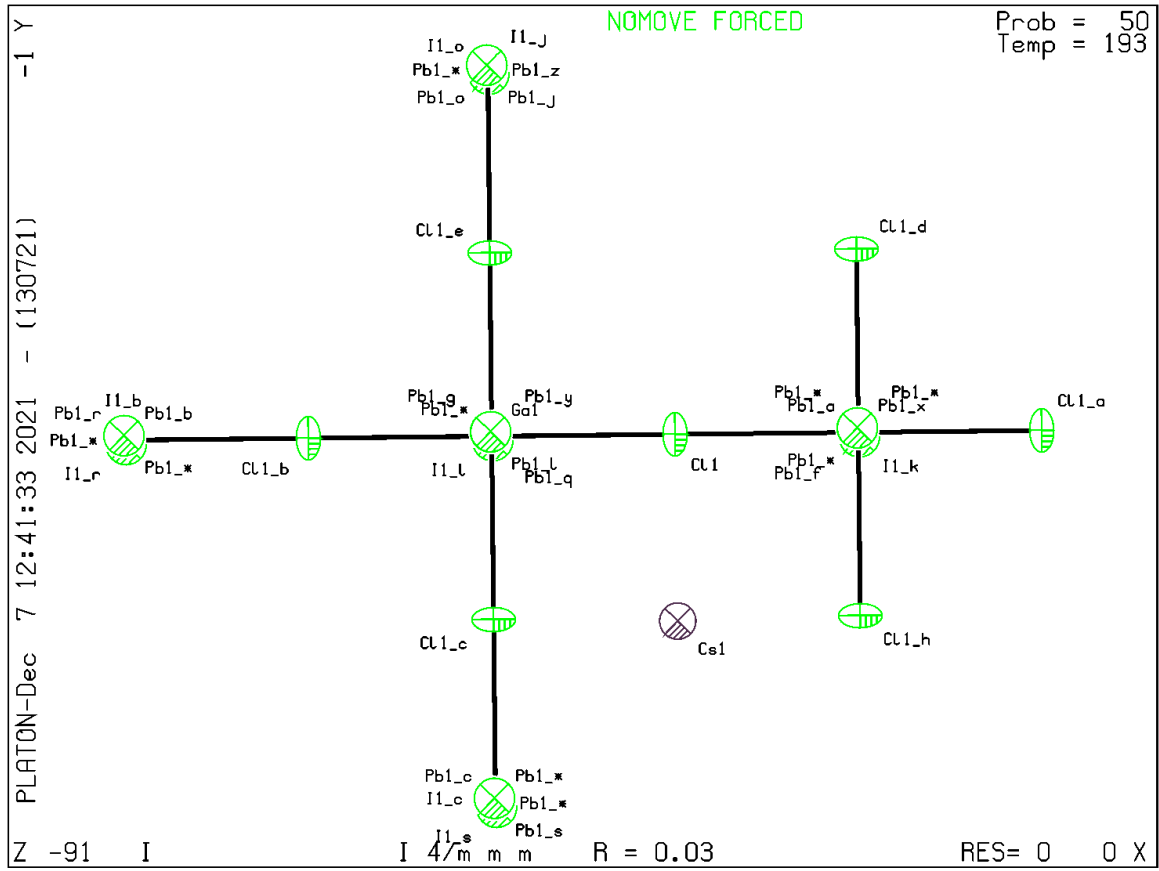
```

# start Validation Reply Form
_vrf_PUBL004_GLOBAL
;
PROBLEM: The contact author's name and address are missing,
RESPONSE: ...
;
_vrf_PUBL005_GLOBAL
;
PROBLEM: _publ_contact_author_email, _publ_contact_author_fax and
RESPONSE: ...
;
_vrf_PUBL006_GLOBAL
;
PROBLEM: _publ_requested_journal is missing
RESPONSE: ...
;
_vrf_PUBL008_GLOBAL
;
PROBLEM: _publ_section_title is missing. Title of paper.
RESPONSE: ...
;
_vrf_PUBL009_GLOBAL
;
PROBLEM: _publ_author_name is missing. List of author(s) name(s).
RESPONSE: ...
;
_vrf_PUBL010_GLOBAL
;
PROBLEM: _publ_author_address is missing. Author(s) address(es).
RESPONSE: ...
;
_vrf_PUBL012_GLOBAL
;
PROBLEM: _publ_section_abstract is missing.
RESPONSE: ...
;
_vrf_PLAT973_I
;
PROBLEM: Check Calcd Positive Resid. Density on          Pb1          3.09 eA-3
RESPONSE: ...
;
# end Validation Reply Form

```

If you wish to submit your CIF for publication in Acta Crystallographica Section C or E, you should upload your CIF via [the web](#). If you wish to submit your CIF for publication in IUCrData you should upload your CIF via [the web](#). If your CIF is to form part of a submission to another IUCr journal, you will be asked, either during electronic [submission](#) or by the Co-editor handling your paper, to upload your CIF via our web site.

Datablock I - ellipsoid plot




The following ALERTS were generated. Each ALERT has the format

test-name_ALERT_alert-type_alert-level.

Click on the hyperlinks for more details of the test.

 **Alert level B**

PLAT911_ALERT_3_B	Missing FCF Refl Between Thmin & STh/L=	0.600	28	Report
PLAT971_ALERT_2_B	Check Calcd Resid. Dens.	0.59A From Pb1	3.06	eA-3

 **Alert level C**

PLAT077_ALERT_4_C	Unitcell Contains Non-integer Number of Atoms ..		Please	Check
PLAT241_ALERT_2_C	High 'MainMol' Ueq as Compared to Neighbors of		I1	Check
PLAT241_ALERT_2_C	High 'MainMol' Ueq as Compared to Neighbors of		C11	Check
PLAT913_ALERT_3_C	Missing # of Very Strong Reflections in FCF		16	Note
PLAT971_ALERT_2_C	Check Calcd Resid. Dens.	0.89A From Pb1	1.76	eA-3
PLAT972_ALERT_2_C	Check Calcd Resid. Dens.	0.66A From Pb1	-1.90	eA-3
PLAT972_ALERT_2_C	Check Calcd Resid. Dens.	0.38A From I1	-1.63	eA-3
PLAT972_ALERT_2_C	Check Calcd Resid. Dens.	0.54A From Cs1	-1.62	eA-3
PLAT974_ALERT_2_C	Check Calcd Negative Resid. Density on	Cs1	-1.11	eA-3

 **Alert level G**

PLAT003_ALERT_2_G	Number of Uiso or Uij Restrained non-H Atoms ...		2	Report
PLAT004_ALERT_5_G	Polymeric Structure Found with Maximum Dimension		2	Info
PLAT019_ALERT_1_G	_diffrn_measured_fraction_theta_full/*_max < 1.0		0.913	Report
PLAT042_ALERT_1_G	Calc. and Reported Moiety Formula Strings Differ		Please	Check
PLAT045_ALERT_1_G	Calculated and Reported Z Differ by a Factor ...		0.50	Check
PLAT068_ALERT_1_G	Reported F000 Differs from Calcd (or Missing)...		Please	Check
PLAT177_ALERT_4_G	The CIF-Embedded .res File Contains DELU Records		1	Report
PLAT178_ALERT_4_G	The CIF-Embedded .res File Contains SIMU Records		1	Report
PLAT300_ALERT_4_G	Atom Site Occupancy of Pb1	Constrained at	0.9499	Check
PLAT300_ALERT_4_G	Atom Site Occupancy of In1	Constrained at	0.0501	Check
PLAT301_ALERT_3_G	Main Residue Disorder(Resd 1)		72%	Note
PLAT860_ALERT_3_G	Number of Least-Squares Restraints		6	Note
PLAT910_ALERT_3_G	Missing # of FCF Reflection(s) Below Theta(Min).		2	Note
PLAT912_ALERT_4_G	Missing # of FCF Reflections Above STh/L=	0.600	3	Note

- 0 **ALERT level A** = Most likely a serious problem - resolve or explain
2 **ALERT level B** = A potentially serious problem, consider carefully
9 **ALERT level C** = Check. Ensure it is not caused by an omission or oversight
14 **ALERT level G** = General information/check it is not something unexpected

- 4 ALERT type 1 CIF construction/syntax error, inconsistent or missing data
9 ALERT type 2 Indicator that the structure model may be wrong or deficient
5 ALERT type 3 Indicator that the structure quality may be low
6 ALERT type 4 Improvement, methodology, query or suggestion
1 ALERT type 5 Informative message, check
-

checkCIF publication errors

Alert level A

PUBL004_ALERT_1_A The contact author's name and address are missing, `_publ_contact_author_name` and `_publ_contact_author_address`.
PUBL005_ALERT_1_A `_publ_contact_author_email`, `_publ_contact_author_fax` and `_publ_contact_author_phone` are all missing.
At least one of these should be present.
PUBL006_ALERT_1_A `_publ_requested_journal` is missing
e.g. 'Acta Crystallographica Section C'
PUBL008_ALERT_1_A `_publ_section_title` is missing. Title of paper.
PUBL009_ALERT_1_A `_publ_author_name` is missing. List of author(s) name(s).
PUBL010_ALERT_1_A `_publ_author_address` is missing. Author(s) address(es).
PUBL012_ALERT_1_A `_publ_section_abstract` is missing.
Abstract of paper in English.

Alert level G

PUBL017_ALERT_1_G The `_publ_section_references` section is missing or empty.

7 **ALERT level A** = Data missing that is essential or data in wrong format
1 **ALERT level G** = General alerts. Data that may be required is missing

Publication of your CIF

You should attempt to resolve as many as possible of the alerts in all categories. Often the minor alerts point to easily fixed oversights, errors and omissions in your CIF or refinement strategy, so attention to these fine details can be worthwhile. In order to resolve some of the more serious problems it may be necessary to carry out additional measurements or structure refinements. However, the nature of your study may justify the reported deviations from journal submission requirements and the more serious of these should be commented upon in the discussion or experimental section of a paper or in the "special_details" fields of the CIF. *checkCIF* was carefully designed to identify outliers and unusual parameters, but every test has its limitations and alerts that are not important in a particular case may appear. Conversely, the absence of alerts does not guarantee there are no aspects of the results needing attention. It is up to the individual to critically assess their own results and, if necessary, seek expert advice.

If level A alerts remain, which you believe to be justified deviations, and you intend to submit this CIF for publication in a journal, you should additionally insert an explanation in your CIF using the Validation Reply Form (VRF) below. This will allow your explanation to be considered as part of the review process.

Validation response form

Please find below a validation response form (VRF) that can be filled in and pasted into your CIF.

```

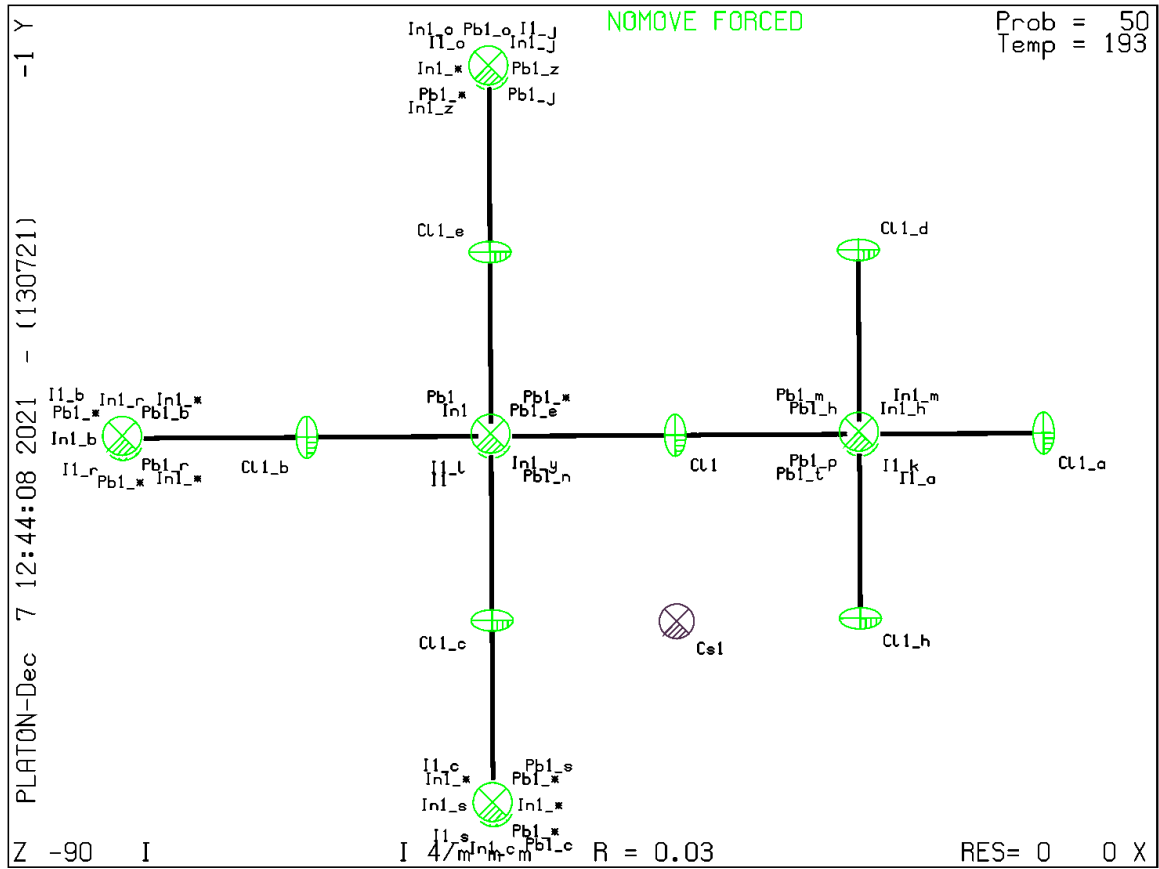
# start Validation Reply Form
_vrf_PUBL004_GLOBAL
;
PROBLEM: The contact author's name and address are missing,
RESPONSE: ...
;
_vrf_PUBL005_GLOBAL
;
PROBLEM: _publ_contact_author_email, _publ_contact_author_fax and
RESPONSE: ...
;
_vrf_PUBL006_GLOBAL
;
PROBLEM: _publ_requested_journal is missing
RESPONSE: ...
;
_vrf_PUBL008_GLOBAL
;
PROBLEM: _publ_section_title is missing. Title of paper.
RESPONSE: ...
;
_vrf_PUBL009_GLOBAL
;
PROBLEM: _publ_author_name is missing. List of author(s) name(s).
RESPONSE: ...
;
_vrf_PUBL010_GLOBAL
;
PROBLEM: _publ_author_address is missing. Author(s) address(es).
RESPONSE: ...
;
_vrf_PUBL012_GLOBAL
;
PROBLEM: _publ_section_abstract is missing.
RESPONSE: ...
;
# end Validation Reply Form

```

If you wish to submit your CIF for publication in Acta Crystallographica Section C or E, you should upload your CIF via [the web](#). If you wish to submit your CIF for publication in IUCrData you should upload your CIF via [the web](#). If your CIF is to form part of a submission to another IUCr journal, you will be asked, either during electronic [submission](#) or by the Co-editor handling your paper, to upload your CIF via our web site.

PLATON version of 13/07/2021; check.def file version of 13/07/2021

Datablock I - ellipsoid plot



The following ALERTS were generated. Each ALERT has the format

test-name_ALERT_alert-type_alert-level.

Click on the hyperlinks for more details of the test.

 **Alert level B**

PLAT911_ALERT_3_B	Missing FCF Refl Between Thmin & STh/L=	0.600	38	Report
PLAT940_ALERT_3_B	Fsqd Refinement With I > n * Sigma(I) Only		Please Check

 **Alert level C**

PLAT077_ALERT_4_C	Unitcell Contains Non-integer Number of Atoms	..		Please Check
PLAT241_ALERT_2_C	High 'MainMol' Ueq as Compared to Neighbors of		I1	Check
PLAT241_ALERT_2_C	High 'MainMol' Ueq as Compared to Neighbors of		C11	Check
PLAT910_ALERT_3_C	Missing # of FCF Reflection(s) Below Theta(Min).		5	Note
PLAT913_ALERT_3_C	Missing # of Very Strong Reflections in FCF	30	Note
PLAT974_ALERT_2_C	Check Calcd Negative Resid. Density on	Cs2	-1.35	eA-3
PLAT974_ALERT_2_C	Check Calcd Negative Resid. Density on	Pb1	-1.20	eA-3
PLAT974_ALERT_2_C	Check Calcd Negative Resid. Density on	Bi1	-1.20	eA-3

 **Alert level G**

PLAT003_ALERT_2_G	Number of Uiso or Uij Restrained non-H Atoms	...	2	Report
PLAT004_ALERT_5_G	Polymeric Structure Found with Maximum Dimension		2	Info
PLAT019_ALERT_1_G	_diffn_measured_fraction_theta_full/*_max < 1.0		0.864	Report
PLAT042_ALERT_1_G	Calc. and Reported Moiety Formula Strings Differ			Please Check
PLAT045_ALERT_1_G	Calculated and Reported Z Differ by a Factor	...	0.50	Check
PLAT177_ALERT_4_G	The CIF-Embedded .res File Contains DELU Records		1	Report
PLAT178_ALERT_4_G	The CIF-Embedded .res File Contains SIMU Records		1	Report
PLAT180_ALERT_4_G	Check Cell Rounding: # of Values Ending with 0 =		3	Note
PLAT300_ALERT_4_G	Atom Site Occupancy of Pb1	Constrained at	0.9499	Check
PLAT300_ALERT_4_G	Atom Site Occupancy of Bi1	Constrained at	0.0501	Check
PLAT301_ALERT_3_G	Main Residue Disorder	(Resd 1)	72%	Note
PLAT802_ALERT_4_G	CIF Input Record(s) with more than 80 Characters		1	Info
PLAT860_ALERT_3_G	Number of Least-Squares Restraints		6	Note
PLAT912_ALERT_4_G	Missing # of FCF Reflections Above STh/L=	0.600	1	Note
PLAT961_ALERT_5_G	Dataset Contains no Negative Intensities		Please Check

0 **ALERT level A** = Most likely a serious problem - resolve or explain
2 **ALERT level B** = A potentially serious problem, consider carefully
8 **ALERT level C** = Check. Ensure it is not caused by an omission or oversight
15 **ALERT level G** = General information/check it is not something unexpected

3 ALERT type 1 CIF construction/syntax error, inconsistent or missing data
6 ALERT type 2 Indicator that the structure model may be wrong or deficient
6 ALERT type 3 Indicator that the structure quality may be low
8 ALERT type 4 Improvement, methodology, query or suggestion
2 ALERT type 5 Informative message, check

checkCIF publication errors

Alert level A

PUBL004_ALERT_1_A The contact author's name and address are missing, `_publ_contact_author_name` and `_publ_contact_author_address`.
PUBL005_ALERT_1_A `_publ_contact_author_email`, `_publ_contact_author_fax` and `_publ_contact_author_phone` are all missing.
At least one of these should be present.
PUBL006_ALERT_1_A `_publ_requested_journal` is missing
e.g. 'Acta Crystallographica Section C'
PUBL008_ALERT_1_A `_publ_section_title` is missing. Title of paper.
PUBL009_ALERT_1_A `_publ_author_name` is missing. List of author(s) name(s).
PUBL010_ALERT_1_A `_publ_author_address` is missing. Author(s) address(es).
PUBL012_ALERT_1_A `_publ_section_abstract` is missing.
Abstract of paper in English.

Alert level G

PUBL017_ALERT_1_G The `_publ_section_references` section is missing or empty.

7 **ALERT level A** = Data missing that is essential or data in wrong format

1 **ALERT level G** = General alerts. Data that may be required is missing

Publication of your CIF

You should attempt to resolve as many as possible of the alerts in all categories. Often the minor alerts point to easily fixed oversights, errors and omissions in your CIF or refinement strategy, so attention to these fine details can be worthwhile. In order to resolve some of the more serious problems it may be necessary to carry out additional measurements or structure refinements. However, the nature of your study may justify the reported deviations from journal submission requirements and the more serious of these should be commented upon in the discussion or experimental section of a paper or in the "special_details" fields of the CIF. *checkCIF* was carefully designed to identify outliers and unusual parameters, but every test has its limitations and alerts that are not important in a particular case may appear. Conversely, the absence of alerts does not guarantee there are no aspects of the results needing attention. It is up to the individual to critically assess their own results and, if necessary, seek expert advice.

If level A alerts remain, which you believe to be justified deviations, and you intend to submit this CIF for publication in a journal, you should additionally insert an explanation in your CIF using the Validation Reply Form (VRF) below. This will allow your explanation to be considered as part of the review process.

Validation response form

Please find below a validation response form (VRF) that can be filled in and pasted into your CIF.

```
# start Validation Reply Form
_vrf_PUBL004_GLOBAL
;
PROBLEM: The contact author's name and address are missing,
RESPONSE: ...
;
_vrf_PUBL005_GLOBAL
;
PROBLEM: _publ_contact_author_email, _publ_contact_author_fax and
RESPONSE: ...
;
_vrf_PUBL006_GLOBAL
;
PROBLEM: _publ_requested_journal is missing
RESPONSE: ...
;
_vrf_PUBL008_GLOBAL
;
PROBLEM: _publ_section_title is missing. Title of paper.
RESPONSE: ...
;
_vrf_PUBL009_GLOBAL
;
PROBLEM: _publ_author_name is missing. List of author(s) name(s).
RESPONSE: ...
;
_vrf_PUBL010_GLOBAL
;
PROBLEM: _publ_author_address is missing. Author(s) address(es).
RESPONSE: ...
;
_vrf_PUBL012_GLOBAL
;
PROBLEM: _publ_section_abstract is missing.
RESPONSE: ...
;
# end Validation Reply Form
```

If you wish to submit your CIF for publication in Acta Crystallographica Section C or E, you should upload your CIF via [the web](#). If you wish to submit your CIF for publication in IUCrData you should upload your CIF via [the web](#). If your CIF is to form part of a submission to another IUCr journal, you will be asked, either during electronic [submission](#) or by the Co-editor handling your paper, to upload your CIF via our web site.

PLATON version of 13/07/2021; check.def file version of 13/07/2021

Datablock I - ellipsoid plot

